JOURNAL OF GEOPHYSICAL RESEARCH, VOL. 103, NO. A8, PAGES 17,705–17,728, AUGUST 1, 1998

Current understanding of magnetic storms: Storm-substorm relationships

Y. Kamide,[1] W. Baumjohann,[2] I. A. Daglis,[3] W. D. Gonzalez,[1, 4] M. Grande,[5] J. A. Joselyn,[6] R. L. McPherron,[7] J. L. Phillips,[8] E. G. D. Reeves,[9] G. Rostoker,[10] A. S. Sharma,[11] H. J. Singer,[6] B. T. Tsurutani,[12] and V. M. Vasyliunas[13]

Abstract. This paper attempts to summarize the current understanding of the storm/substorm relationship by clearing up a considerable amount of controversy and by addressing the question of how solar wind energy is deposited into and is dissipated in the constituent elements that are critical to magnetospheric and ionospheric processes during magnetic storms. (1) Four mechanisms are identified and discussed as the primary causes of enhanced electric fields in the interplanetary medium responsible for geomagnetic storms. It is pointed out that in reality, these four mechanisms, which are not mutually exclusive, but interdependent, interact differently from event to event. Interplanetary coronal mass ejections (ICMEs) and corotating interaction regions (CIRs) are found to be the primary phenomena responsible for the main phase of geomagnetic storms. The other two mechanisms, i.e., HILDCAA (high-intensity, long-duration, continuous auroral electrojet activity) and the so-called Russell-McPherron effect, work to make the ICME and CIR phenomena more geoeffective. The solar cycle dependence of the various sources in creating magnetic storms has yet to be quantitatively understood. (2) A serious controversy exists as to whether the successive occurrence of intense substorms plays a direct role in the energization of ring current particles or whether the enhanced electric field associated with southward IMF enhances the effect of substorm expansions. While most of the *Dst* variance during magnetic storms can be solely reproduced by changes in the large-scale electric field in the solar wind and the residuals are uncorrelated with substorms, recent satellite observations of the ring current constituents during the main phase of magnetic storms show the importance of ionospheric ions. This implies that ionospheric ions, which are associated with the frequent occurrence of intense substorms, are accelerated upward along magnetic field lines, contributing to the energy density of the storm-time ring current. An apparently new controversy regarding the relative importance of the two processes is thus created. It is important to identify the role of substorm occurrence in the large-scale enhancement of magnetospheric convection driven by solar wind electric fields. (3) Numerical schemes for predicting geomagnetic activity indices on the basis of solar/solar wind/interplanetary magnetic field parameters continue to be upgraded, ensuring reliable techniques for forecasting magnetic storms under real-time conditions. There is a need to evaluate the prediction capability of geomagnetic indices on the basis of physical processes that occur during storm time substorms. (4) It is crucial to differentiate between storms and nonstorm time substorms in terms of energy transfer/conversion processes, i.e., mechanical energy from the solar wind, electromagnetic energy in the magnetotail, and again, mechanical energy of particles in the plasma sheet, ring current, and aurora. To help answer the question of the role of substorms in energizing ring current particles, it is crucial to find efficient magnetospheric processes that heat ions up to some minimal energies so that they can have an effect on the strength of the storm time ring current. (5) The question of whether the *Dst* index is an accurate and effective measure of the storm time ring current is also controversial. In particular, it is demonstrated that the dipolarization effect associated with substorm expansion acts to reduce the *Dst* magnitude, even though the ring current may still be growing.

[1] Solar-Terrestrial Environment Laboratory, Nagoya University, Toyokawa, Japan.

[2] Max-Planck-Institut für extraterrestrische Physik, Garching, Germany.

[3] Institute of Ionospheric and Space Research, National Observatory of Athens, Penteli, Greece.

[4] Permanently at Instituto de Pesquisas Espaciais, São José dos Campos, São Paulo, Brazil.

[5] Rutherford Appleton Laboratory, Chilton, Didcot, Oxon, England.

[6] Space Environment Center, NOAA, Boulder, Colorado.

[7] Institute of Geophysics and Planetary Physics, University of California, Los Angeles.

Paper number 98JA01426.
0148-0227/98/98JA-01426$09.00

[8] NASA Johnson Space Flight Center, Houston, Texas.

[9] Los Alamos National Laboratory, Los Alamos, New Mexico.

[10] Department of Physics, University of Alberta, Edmonton, Alberta, Canada.

[11] Department of Astronomy, University of Maryland, College Park.

[12] Jet Propulsion Laboratory, California Institute of Technology, Pasadena.

[13] Max-Planck-Institut für Aeronomie, Katlenburg-Lindau, Germany.

1. Introduction: What is a Geomagnetic Storm?

Geomagnetic storms were first defined by researchers looking at ground magnetograms recorded at relatively low geomagnetic latitudes. It is not too much of an exaggeration to state that the challenge facing modern space physics, i.e., the dynamics of the

solar-terrestrial environment, originated in the study of geomagnetic storms. It was in the mid-1800s that extraordinary disturbances and a great decrease in the horizontal component of the earth's magnetic field were coined, "geomagnetic storms" or "magnetic storms" [see *Chapman and Bartels*, 1940].

The characteristic signature of a magnetic storm is a depression in the H component of the magnetic field lasting over some tens of hours. This depression is caused by the ring current encircling the Earth in the westward direction and can be monitored by the *Dst* index. It is now commonly assumed that the magnitude of magnetic storms can be defined by the minimum *Dst* value [*Gonzalez et al.*, 1994]. In the early years of research, a general picture of a typical magnetic storm emerged that had the features shown in Figure 1. The picture of the storm involved a sudden positive increase in the H component (sudden storm commencement or SSC) followed by a period of arbitrary length in which the elevated field did not change significantly (the initial phase). This was followed by the development of a depressed H component (the main phase) transpiring over a period from one to a few hours. The storm concluded by a slow recovery over hours to tens of hours (the recovery phase).

The SSC was understood as early as the 1930s [*Chapman and Ferraro*, 1931] as being the effect of a compression of the front side of the magnetosphere by enhanced solar wind pressure. The depression of the magnetic field during the main phase was explained by *Singer* [1957] as the effect of a ring current carried primarily by energetic ions [e.g., *Frank*, 1967; *Smith and Hoffman*, 1973] which appeared in the region of $L \sim 4$ - 6 during the growth of the storm main phase and decayed due to charge exchange, Coulomb interaction and wave-particle interaction processes in the volume of space occupied by the ring current particles [see, e.g., *Prölss*, 1973; *Kozyra et al.*, 1997].

In due course it was discovered that the direction of the north-south component of the interplanetary magnetic field (IMF) regulated the growth of the ring current. In fact, it became possible to model successfully the growth of the ring current using, as input, only the component of the interplanetary electric field in the ecliptic plane normal to the Sun-Earth line [see *Burton et al.*, 1975; *Gonzalez et al.*, 1989]. By that time, several things were becoming clear about the essence of a geomagnetic storm. First, it was recognized [*Rostoker and Fälthammar*, 1967] that the initial phase simply represented a period of time after the onset of the SSC during which the IMF was oriented primarily northward (i.e., little energy was entering the magnetosphere regardless of the speed and number density of particles in the solar wind). More importantly, it was discovered that an SSC is not a necessary condition for a storm to occur, and hence the initial phase is not an essential feature [see *Akasofu*, 1965; *Joselyn and Tsurutani*, 1990]. In fact, the only essential feature of a storm is the significant development of a ring current and its subsequent decay.

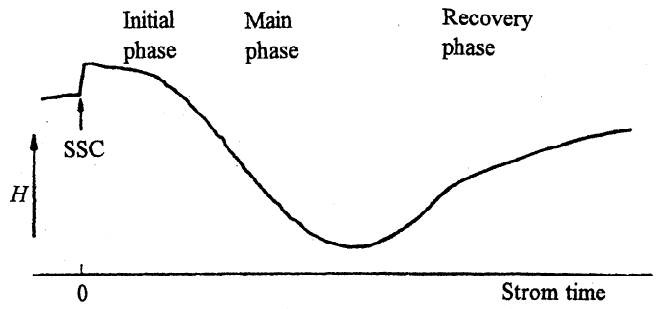

Figure 1. Schematic diagram of *Dst* featuring a typical geomagnetic storm. For the definition of the initial, main, and recovery phases, see text.

The main question that then arises regarding magnetic storms involves the nature of the physical processes that lead to the growth and decay of the ring current. This question was apparently answered by *Akasofu and Chapman* [1961] who noted that during the main phase of a storm, there was violent electrojet activity in the midnight sector auroral oval with the amplitudes of the disturbances there far exceeding the magnetic perturbation associated with the ring current itself. These auroral oval disturbances, i.e., polar substorms, were in some way thought to be responsible for the growth of the ring current. In fact, early studies of energetic particle "injections" into the region of geostationary orbit by *Akasofu et al.* [1974] strongly suggested that substorms led to the acceleration of particles to energies that allowed them to be effective current carriers in the ring current. However, it later became clear that the storm time ring current was carried by energetic ions with energies typically in excess of several tens of keV [see *Williams*, 1980, 1987]. The question of how ring current particles attain their energies and whether substorm disturbances play an integral role in that process is still open.

In recent times it has become clear that during geomagnetic storms, significant amounts of atomic oxygen are transferred from the auroral ionosphere into the plasma sheet [*Balsiger et al.*, 1972] and ultimately form a significant component of the ring current population [*Johnson et al.*, 1977; *Daglis*, 1997]. Since charge exchange processes affect oxygen ions and protons differently in terms of decay times, the observed decay of the ring current can reflect the different behavior of the components of the ring current due to the two ion species [see, e.g., *Kozyra et al.*, 1997]. It is important to evaluate the importance of ring current composition in terms of the differing signatures of ring current decay seen using ground magnetic observatories. In other words, the relationship between substorms and storms is currently poorly understood, and therefore basic questions remain unanswered regarding the hypothesis of whether a magnetic storm is a superposition of intense substorms [*Akasofu*, 1968].

Motivated by these timely issues about storm/substorm relationships, the authors of this paper met in Rikubetsu, Hokkaido, Japan, in October 1994 and in Lake Arrowhead, California, in February 1996 to address the questions and also to attempt to clear up a considerable amount of confusion in the field. The authors believe that it might be instructive to publish the result of the two workshops and of further elaboration, summarizing the current understanding of geomagnetic storms, particularly of storm/substorm relationships.

2. Solar Wind Conditions Leading to Magnetic Storms

The precise form of the input function for solar wind energy into the magnetosphere has been debated in countless papers, without the emergence of a true consensus. However, the evidence is overwhelming that solar wind dawn-to-dusk electric fields directly drive magnetospheric convection [e.g., *Kamide*, 1992; *Gonzalez et al.*, 1994]. These electric fields are caused by a combination of solar wind velocity and southward IMF. Of these two parameters, the southward field is probably the more important because of its far greater variability [*Tsurutani et al.*, 1992]. Solar wind ram pressure is also important in ring current energization, although perhaps less so in auroral processes [*Gonzalez et al.*, 1989]. In this section, the specific circumstances or solar wind conditions typically leading to enhanced duskward electric fields of substantial duration will first be described briefly, accompanied by two examples which illustrate most of the major effects, followed by a discussion of the interactions and specific roles of these conditions.

The dominant solar/coronal events that occur near the maximum sunspot phase of the solar cycle are impulsive ejecta,

often called coronal mass ejections (CMEs). Mass ejections are distinct particle and field structures with field orientations not generally favoring the typical spiral equatorial orientation [e.g., *Gonzalez and Tsurutani*, 1987; *Gosling et al.*, 1987]. CMEs are most numerous near solar maximum [*Webb and Howard*, 1994], and have been demonstrated to cause most major geomagnetic storms at that phase of the solar cycle and possibly at other phases as well [e.g., *Gosling et al.*, 1991; *Taylor et al.*, 1994]. These events have a variety of speeds, but it has been statistically shown that the ones that are most effective in creating magnetic storms are events that are fast, with speeds exceeding the ambient wind speed by the magnetosonic wave speed, so that a fast forward shock is formed [*Gosling et al.*, 1991; *Phillips et al.*, 1993]. As a fast plasma and field structure propagates from the Sun through interplanetary space, it sweeps up and compresses the slower plasma and field ahead, creating a "sheath" between the shock and the interplanetary manifestation of the ejecta. There are three prominent features of CMEs observed near the Sun: bright outer loops, a dark region, and filamentary structures near the coronal base. It is not clear that all propagate into interplanetary space [*Tsurutani and Gonzalez*, 1997].

Figure 2 illustrates the schematic of the regions of possible intense IMF for such solar ejecta, i.e., driver gas, detected at 1 AU: see *Tsurutani and Gonzalez* [1995] for details. Two types of satellite crossings are shown. The sheath fields leading the fast ejecta often contain substantial north-south field components, possibly due to compression and draping of the ambient IMF over the ICMEs (interplanetary CMEs) [*Tsurutani et al.*, 1988; *McComas et al.*, 1989; *Zhao et al.*, 1993]. Both the remnant ejecta fields and plasma and those of the sheath can be geoeffective, depending on the field orientations [*Tsurutani et al.*, 1988; *Zhao et al.*, 1993]. It should be noted that roughly five out of six fast ejecta do not cause $Dst < -100$ nT storms, because they lack large southward field components persisting for three hours or longer [*Tsurutani et al.*, 1996]. Most geoeffective ICMEs are magnetic clouds [*Klein and Burlaga*, 1982; *Farrugia et al.*, 1997], a subset of ejecta characterized by high IMF magnitude, low field variance, and large-scale coherent field rotations, often

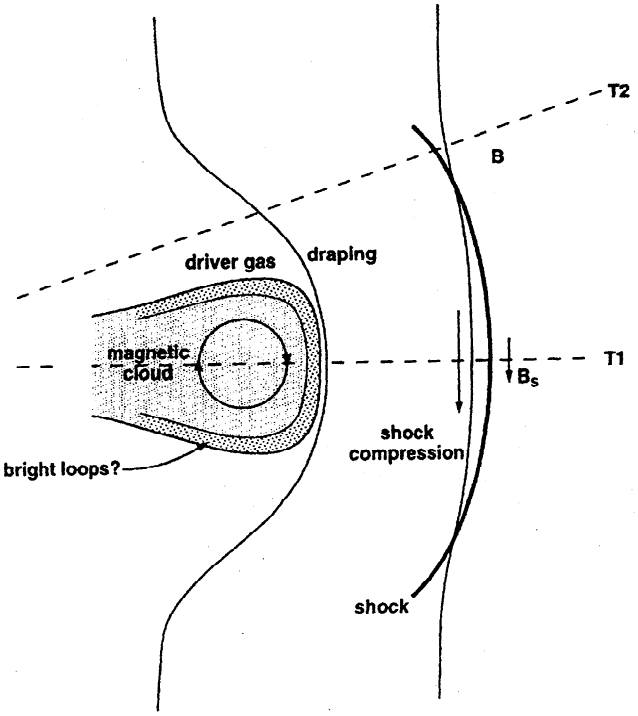

Figure 2. Schematic of regions of intense IMF seen during solar maximum. T1 and T2 are two types of satellite crossings in the interplanetary structure.

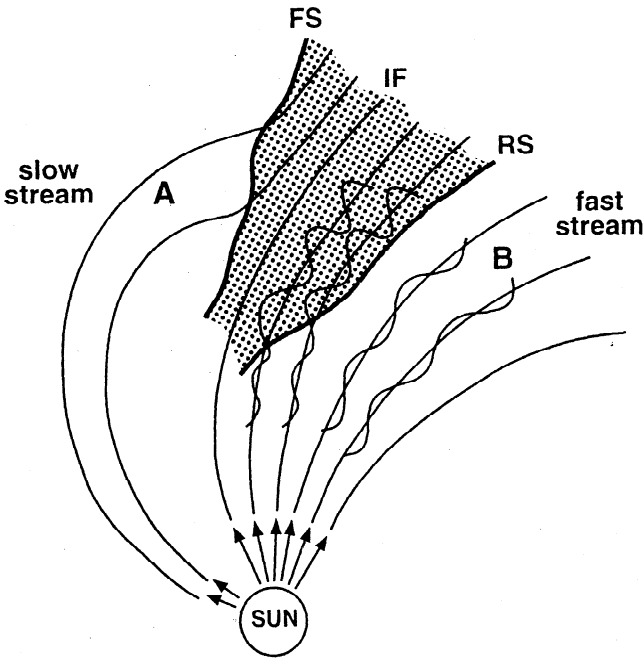

Figure 3. Schematic of the formation of corotating interaction regions (CIRs) during the descending phase of the solar cycle. The interaction between a high-speed stream (B) and a slow-speed stream (A) are shown together with the CIR (shaded). The forward shock (FS), interface surface (IF), and reverse shock (RS) are also indicated.

including large and steady north-south components. This high field region is typically a low beta plasma. The field reversals typical within magnetic clouds feature magnetic field reconnection during the period of southward field and a general lack of reconnection and solar wind injection into the magnetosphere during the part with northward field [*Tsurutani and Gonzalez*, 1995]. The storm initial phase is created by the increased ram pressure behind the fast shock. The higher plasma density and higher velocity combine to form a much larger solar wind ram pressure. This pressure compresses the Earth's magnetosphere and increases the field magnitude near the equator. Since interplanetary shocks are thin discontinuities, they create an abrupt onset of the initial phase, and what has been called an SSC.

However, as mentioned above, there is no guarantee that southward magnetic field events will follow the shock and therefore a storm main phase may not follow the SSC. If there are intense, long-duration southward field intervals in either the sheath or the ejecta proper, a main phase may follow.

During the declining phase of the solar cycle, another type of solar/coronal event dominates. During this phase, the coronal holes have expanded from polar locations and extend into, and sometimes across, the equatorial regions. Recent Ulysses observations have shown that fast (750-800 km/s), tenuous plasma is continuously emitted from these solar regions [e.g., *Phillips et al.*, 1995]. Because these regions are long-lived and evolve relatively slowly, they appear to "corotate" with the Sun (a 27-day period as observed from Earth). If a coronal hole is near the ecliptic plane, the Earth's magnetosphere will be bathed in this stream once per solar rotation. Typically, a heliospheric neutral sheet/plasma sheet lies ahead of the fast stream in interplanetary space [*Winterhalter et al.*, 1994]. The characteristics of the plasma sheet wind include low speed (~350 km/s) and high density (tens of particles/cm^3). The interaction of the fast stream with the slow stream ahead creates a plasma and field

compression called a corotating interaction region (CIR) [*Smith and Wolfe*, 1976]. CIRs are bounded on the leading and trailing edges by forward- and reverse-propagating compressional waves, respectively. CIRs are not as well-developed at 1 AU as they are at greater heliocentric distances. The reverse waves sometimes steepen into shocks by 1 AU, while the forward waves rarely do so, and the magnetic field and density profiles within the compressed regions are often irregular. Figure 3 shows schematically the formation of CIRs in which magnetic field fluctuations are present in the high speed stream proper.

A 27-day modulation in geomagnetic activity has been noted since the 19th century [see *Crooker and Cliver*, 1994, for historical references]. This periodicity, attributed to solar regions called "M-regions" by *Bartels* [1932], was later discovered to arise from high-speed solar wind streams originating in coronal holes [*Neupert and Pizzo*, 1974; *Sheeley et al.*, 1976]. However, for the elevated activity levels associated with geomagnetic storms, the picture is somewhat more complicated. While ICMEs often contain sustained southward fields accompanied by fast wind speeds, the high-speed wind from coronal holes generally has relatively low field magnitude and a radial orientation not conducive to production of steady and substantial north-south fields. However, the interaction of this fast wind with slower, denser streamer wind, forming a CIR, produces geoeffective field compressions and deflections. Geomagnetic storms associated with CIR-like plasma signatures rarely have minimum $Dst < -100$ nT, and generally lack the sudden commencements often occurring for ICME-driven storms [*Taylor et al.*, 1994; *Tsurutani et al.*, 1995]. The high densities of the heliospheric plasma sheet wind create increased compression of the magnetosphere, thus an "initial phase" if the period following the shock features northward or weakly southward IMF. However, there is rarely a forward shock and so the compression is gradual, with no "sudden impulse" or SSC. We note that in most cases [*Tsurutani et al.*, 1995], the very high plasma densities associated with the heliospheric plasma sheet can overcome the associated low wind speeds, creating a ram pressure increase and a storm "initial phase" which actually precedes the CIR.

One remarkable characteristic of coronal hole wind is the presence of continuous Alfvénic activity, consisting of large-amplitude quasi-periodic fluctuations in the IMF orientation, in-phase with similar fluctuations in the solar wind flow direction, with periods from tens of minutes to a few hours [*Belcher and Davis*, 1971]. Thus, in the interplanetary region following CIRs, the southward field components caused by these waves can cause magnetic reconnection, small injections of plasma into the magnetosphere, and prolonged recovery phases of the storms. Events of this type are known as "high-intensity, long-duration, continuous *AE* activity" (HILDCAA) events [*Tsurutani and Gonzalez*, 1987]. Although the average B_Z component in HILDCAA intervals is zero, the half-wave induced reconnection in the magnetospheric response [*Gonzalez and Mozer*, 1974] results in a continuous occurrence of substorms.

A final mechanism which may enhance storm activity is based on the simple geometric mapping from the solar equatorial plane, in which the prevailing IMF is ordered, into a magnetospheric system which orders the response. This mapping, from solar equatorial (GSEG) to solar magnetospheric (GSM) coordinates, was described by *Russell and McPherron* [1973]. The result of the offsets between the solar equatorial, ecliptic, and terrestrial rotational planes is to create a seasonal modulation in the rotation from the transverse solar equatorial IMF component (GSEQ B_y) into north-south field in the magnetospheric system (GSM B_z). The tilt of the terrestrial dipole adds a diurnal component. The combined effect is that negative GSEQ B_y, corresponding to "toward sector" IMF, maps most directly to negative GSM B_z at 2200 UT on April 5, while positive GSEQ B_y ("away sector") maps most directly to negative GSM B_z at 1000 UT on October 5.

Figure 4 shows the seasonal pattern in 25- and 75-percentile observed GSM B_z for a full 22-year solar magnetic cycle, for toward and away sectors. Compare the strong seasonal signal in GSM with the lack of modulation in GSEQ coordinates, also shown. The Russell-McPherron effect is often assumed to be responsible for the prevailing seasonal modulation in average geomagnetic activity, with highest activity levels in spring and fall. This modulation has been shown to increase in amplitude with increasing activity threshold [*Green*, 1984] and to persist even for very disturbed geomagnetic conditions [e.g., *Crooker et al.*, 1992]. However, the effectiveness of the Russell-McPherron effect in driving strong geomagnetic storms has been questioned by *Gonzalez et al.* [1993], who argued that the observed field mappings for a set of storms did not fit the predicted pattern [see *Crooker and Cliver*, 1993]. Currently, there is agreement on the effectiveness of this mechanism only for substorms but such an agreement is not clear for magnetic storms.

An example of geomagnetic activity produced by a fast ICME encountered on September 29-30, 1978, is shown in Figure 5. The top three panels show IMF magnitude and selected components, the next three panels show solar wind parameters, and the bottom two show the *Kp* and *Dst* indices, including a corrected (for solar wind dynamic pressure) version of the latter index [e.g., *Gonzalez et al.*, 1989]. A fast forward shock (solid vertical trace) arrived near 2100 UT on September 29, driven by an ICME (dashed vertical traces) which spanned roughly 0830 UT on September 29 through 0300 UT on September 30, as identified by a variety of particle and field signatures. The enhanced *Kp* and depressed *Dst* existing prior to the arrival of the shock/ICME event were caused by an earlier (September 26) ICME [*Gosling et al.*, 1987], augmented by the near-equinoctial timing and the subsequent mapping of positive GSEQ B_y to negative GSM B_z (note that the southward field is slightly stronger in GSM than in GSEQ for all intervals with substantial GSEQ B_y). The field in the "sheath" region between the shock and ICME became strongly southward just prior to ICME arrival, with a resulting enhancement of geomagnetic activity. Within the structure proper, which is a classic magnetic cloud, the field is roughly evenly divided between strongly southward and strongly northward intervals. The geomagnetic indices were at major storm levels during the southward field interval, then began to recover when the field swung northward. Thus the southward fields created large convective electric fields causing the enhanced storm ring current, while the northward fields resulted in geomagnetic quiet. This storm was driven by a fast ICME, augmented by preexisting enhanced geomagnetic activity and by the Russell-McPherron effect.

An example of geomagnetic activity produced by a CIR with a trailing HILDCAA interval is shown in Figure 6, in the same format as Figure 5 and spanning January 24 through 27, 1974. After a geomagnetically quiet interval due to slow solar wind and near-zero north-south field, the leading edge of a CIR arrived during the afternoon of January 24. Field magnitude, plasma density, and wind speed all began to ramp up, while the GSEQ field rotated strongly toward -*Y* and -*Z*. Near the interface between streamer belt (slow) and coronal hole (fast) wind, marked by a vertical dashed trace, the GSEQ field initially rotated northward then turned back southward; the resulting GSM field has both northerly and southerly intervals as well. Geomagnetic activity increased throughout the CIR due to increasing wind speed and intervals of substantial southward field. The CIR ended with a reverse shock (solid vertical trace) late on January 25. Subsequently, the solar wind was fast and low in density, with a steady field magnitude and north-south (GSM) field components which averaged to roughly zero but included

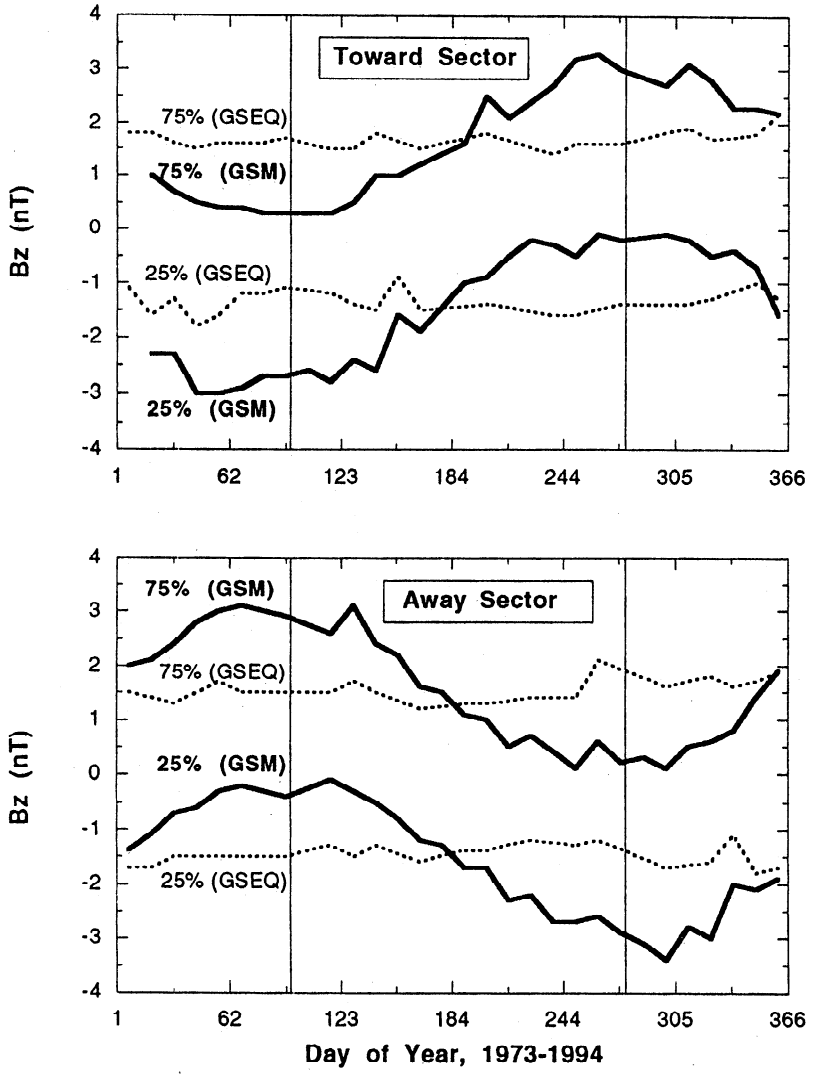

Figure 4. Twenty-five and 75 percentile levels for B_z, in GSEQ and GSM coordinates, plotted versus day of year in 12.2-day bins. Twenty-two years of hourly-averaged NSSDC Omni data were used, spanning 1973-1994. Data were sorted by GSEQ B_x and B_y into (top) toward and (bottom) away sector quadrants; measurements in anomalous nonspiral quadrants were not used. The vertical traces mark the *Russell and McPherron* [1973] "equinoxes" on April 5 and October 5. The diurnal component has been averaged out by including measurements from all times of day.

quasiperiodic large-amplitude north-south oscillations. The result of this Alfvénic (HILDCAA) activity was that recovery from the CIR-driven magnetic storm was delayed for several days. *Dst* did not return to its preevent levels until early on January 28 (not shown).

The four mechanisms described and illustrated above (ICMEs, CIRs, Alfvénic IMF fluctuations, and the Russell-McPherron effect) are the primary causes of the enhanced solar wind electric fields responsible for geomagnetic storms. Of these, ICMEs and CIRs can be considered the primary events driving the storms, while the other two are modifiers which generally do not produce storms without a ICME or CIR. This picture is, however, admittedly oversimplified for illustrative purpose. In reality, these four mechanisms interact differently from event to event. One suggested ramification for seasonal modulation of geomagnetic storms is the "postshock Russell-McPherron effect," originally proposed for shocked solar wind leading ICMEs [*Crooker et al.*, 1992]. In this mechanism, the enhanced field magnitude and transverse orientation in shocked or compressed solar wind can map to strong north-south GSM field. CIRs may also be particularly effective in driving enhanced geomagnetic activity when the IMF polarity and time ~~of~~ year are appropriate for mapping the enhanced transverse fields (GSEQ B_y) within the compression regions to southward (GSM) fields [*Crooker and Cliver*, 1994; *Tsurutani et al.*, 1995].

The existence of a semiannual signal in CIR-driven magnetic storms has been demonstrated by *Taylor et al.* [1996]. That study did not demonstrate explicitly that this signal was driven by the postshock Russell-McPherron effect. *Gonzalez et al.* [1993] concluded that the postshock Russell-McPherron mechanism was ineffective in driving storms during the declining phase of a particular sunspot cycle. However, *Phillips et al.* [1993] observationally confirmed this effect for regions between shocks and fast ICMEs. It seems likely that the Russell-McPherron mechanism is a modifier that enhances the geoeffectiveness of CIRs resulting from (1) compression and (2) HILDCAAs associated with the high-speed wind. While the compressed and draped fields preceding ICMEs are ordered in solar heliographic

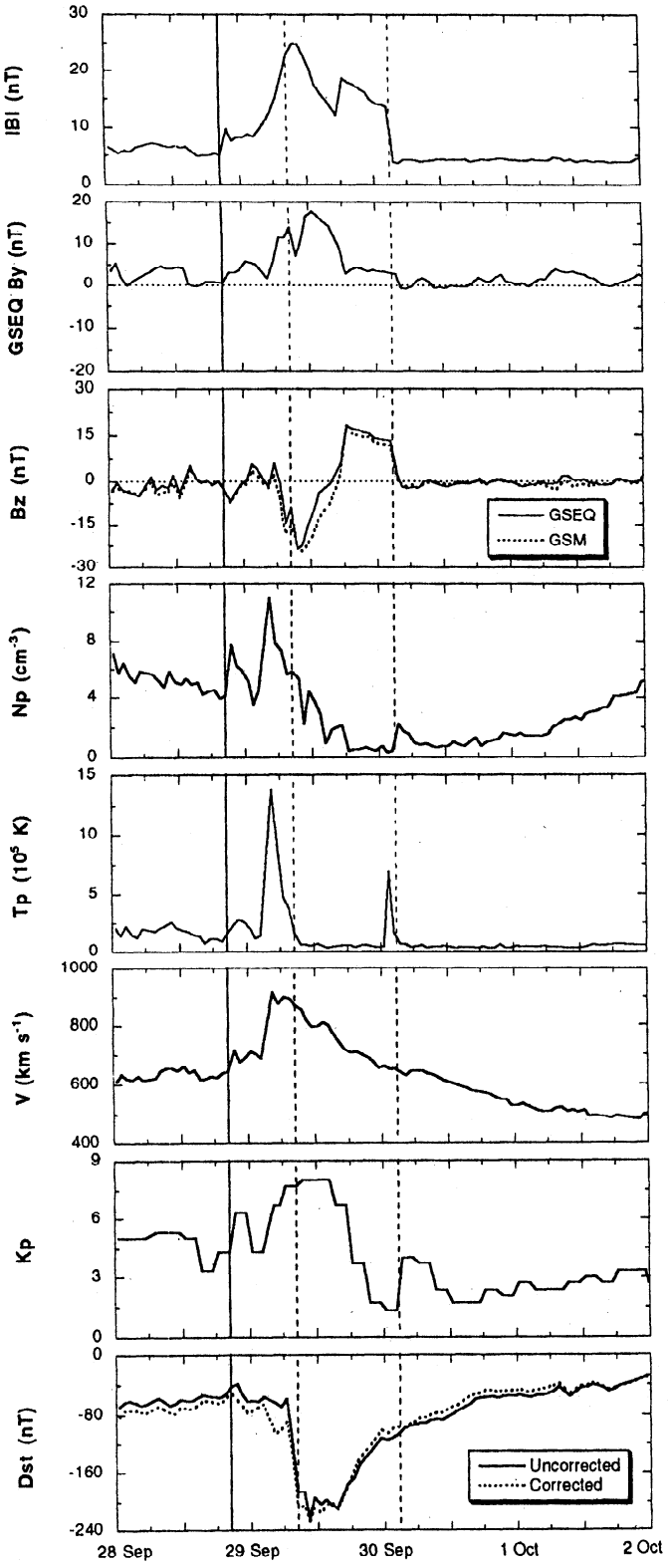

Figure 5. Interplanetary and geomagnetic data for a shock-ICME sequence from September 28 through October 1, 1978. Interplanetary data are 1-hour averages from the NASA NSSDC OMNI data set and are primarily from IMP 8 and ISEE 3, plus a small contribution from ISEE 1. The shock and ICME are marked by solid and dashed vertical traces, respectively.

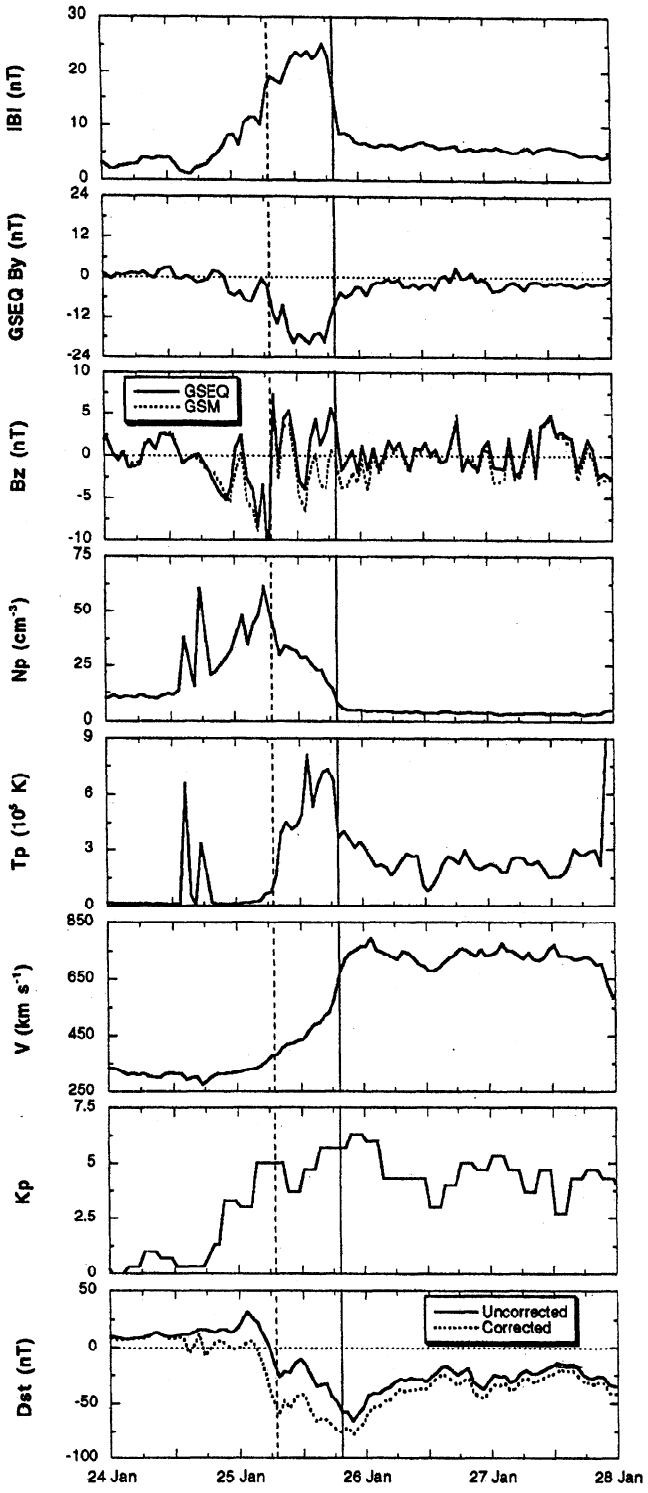

Figure 6. Same format as Figure 6, for a CIR-HILDCAA sequence from January 24 through January 27, 1974. Interplanetary data are 1-hour averages from the NASA NSSDC Omni dataset and represent measurements from IMP 6, 7, 8, and HEOS. The reverse shock and stream interface are marked by solid and dashed vertical traces, respectively.

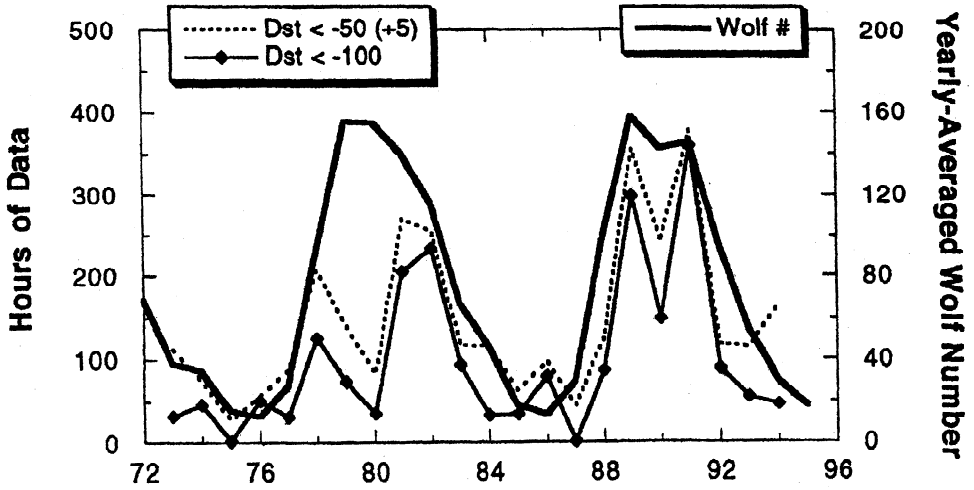

Figure 7. Yearly averaged number of hours with $Dst < -100$ nT (solid trace with diamonds, and with $Dst < -50$ nT (divided by 5, dashed trace), and yearly averaged Wolf number (heavy trace), for a solar magnetic cycle. *Dst* values are from the NSSDC OMNI data set; Wolf numbers are from the NOAA National Geophysical Data Center.

coordinates and thus have a seasonal modulation in geoeffectiveness, the evidence for heliographic ordering of the ejecta fields themselves is less compelling. However, *Zhao et al.* [1993] found that internal ICME field orientation may indeed exhibit a preference for the prevailing solar field pattern, suggesting that these fields also contribute to the seasonal pattern of geomagnetic storms. Recent analysis by *Crooker and Cliver* [1994] suggests that ICMEs may also contribute to enhanced quasiperiodic geomagnetic activity at roughly the solar rotational period in three ways, including (1) clustering of ICMEs near sector boundaries, (2) compression of slow ICMEs within CIRs, and (3) increasing of magnetic flux in the streamer belt.

Consideration of ICMEs and CIRs as the primary drivers for strong geomagnetic activity can at least partly explain the strong solar cycle effect in geomagnetic disturbances. Figure 7 illustrates this effect, showing the yearly averaged Wolf number and the hours of $Dst < -50$ and -100 nT for years 1973 through 1994. Note that the intervals of low *Dst* roughly follow the sunspot cycle, but have pronounced dips during the years of solar magnetic polarity reversal (1980 and 1990), and reach maxima early in the declining phase [cf. *Gonzalez et al.*, 1990]. ICME occurrence rate roughly follows the sunspot cycle [*Webb and Howard*, 1994], while strong CIRs are most prevalent during the declining phase due the relatively large tilt of the heliomagnetic streamer belt and the presence of large polar coronal holes [e.g., *Tsurutani et al.*, 1995]. A superposition of occurrence rates of fast ICMEs and strong CIRs might well produce the double-peaked pattern of Figure 7 [*Webb*, 1995]. These minima could also be caused by differences in the size or speed of ICMEs encountered near sunspot maximum (but see evidence to the contrary by *Hundhausen et al.* [1994]).

Another possible trend in geomagnetic activity is its modulation in accordance with the 22-year Hale cycle. The average geomagnetic activity levels are historically highest during the rising phase of odd-numbered sunspot cycles and during the declining phase of even cycles [e.g., *Cliver et al.*, 1996, and references therein]. Note in Figure 5, however, that this trend is not supported for cycle 21 (1976-1986), which was active during the declining phase (i.e., 1981-1982). Furthermore, studies to date [e.g., *Cliver et al.*, 1996] have generally used the *aa* index or some similar parameter due to its availability for more than 100 years. Evidence for a 22-year period in such an index does not necessarily guarantee similar modulation in ring-current enhancement or in the occurrence of geomagnetic storms. Advocates of the "double-solar-cycle" variation have suggested two sources. The first is a combination of the Russell-McPherron effect, the heliographic latitude dependence of the IMF strength, and the solar magnetic polarity [*Rosenberg and Coleman*, 1969; *Russell and McPherron*, 1973]. The second is an intrinsic difference in large-scale solar magnetic fields, perhaps manifested as changes in the solar wind, between odd and even cycles. Note that the odd- and even-numbered cycles have some differences in average solar wind speed profiles. *Slavin et al.* [1986] noted that the IMF magnitude was substantially higher in cycle 21 than in cycle 20. A variety of evidence favoring intrinsic and systematic differences in solar properties between even and odd cycles was presented by *Cliver et al.* [1996]. We summarize by stating that the case for a 22-year cycle in geomagnetic activity is compelling but not ironclad, that one must be wary of high-latitude evidence for geomagnetic modulation without reference to a true storm parameter, and that various solar and interplanetary mechanisms may be at work to produce the observed effect.

3. Predicting Geomagnetic Storm Development

Quantitative predictions of storm development and decay have progressed considerably since *Russell et al.* [1974] and *Burton et al.* [1975] published an empirical relationship between *Dst* and the product of solar wind V (velocity) and B_s (southward interplanetary magnetic field). A number of data-based techniques useful for magnetic storm forecasting are now available: see *Joselyn* [1995]. Techniques using statistical time series analysis were reviewed by *Baker* [1986]. Linear prediction filters, pioneered by *Iyemori et al.* [1979], have been further developed [e.g., *Clauer*, 1986; *McPherron et al.*, 1986; *Fay et al.*, 1986]. Recently, both linear and nonlinear autoregressive and moving average filters for predicting *Dst*, including local linear prediction (the state space technique) [*Vassiliadis et al.*, 1995] were reviewed and evaluated by *Detman and Vassiliadis* [1997]. *Campbell* [1996] showed that by using measurements made

during the main phase, *Dst* development following the maximum depression could be modeled by assuming a lognormal distribution. *Valdivia et al.* [1996] developed a nonlinear predictive model to predict storm main-phase onset and evolution. Using the solar wind and *Dst* data, it can predict both the main-phase onset as well as its time development. On the other hand, using *Dst* data alone, the model cannot predict the main-phase onset but can predict its time development. Artificial intelligence (AI) mathematical techniques have brought interesting new tools to bear on disparate and asynchronous sets of solar wind, magnetospheric, and ionospheric data [*Wu and Lundstedt*, 1996; *Gleisner and Lundstedt*, 1997; *Lundstedt*, 1997].

Several of these techniques are being implemented and tested for reliability for predicting geomagnetic indices under real-time conditions. These include a linear filter to be used operationally for predicting *Kp* (T. R. Detman, private communication, 1996); a state-space local linear filter for predicting *AL* (D. Vassiliadis, private communication, 1996; http://lep694.gsfc.nasa.gov/code692/vassiliadis/htmls/alprediction.html); an AI technique that will predict *Dst* from continuous real-time solar wind data (H. Lundstedt, private communication, 1996; http://nastol.astro.lu.se/~henrik/spacew1.html); and a nonlinear dynamical prediction of *Dst* from solar wind data (http://spp.astro.umd.edu). An AI technique is used internally in the Magnetospheric Specification and Forecast Model (MSFM) to predict *Dst* [*Freeman et al.*, 1994]. Real-time or near real-time solar wind data are available on two internet sites: (http://www.sec.noaa.gov/wind/rtwind.html) and (http://umtof.umd.edu/pm/). A World Wide Web site at the World Data Center C2 in Kyoto, Japan (http://swdcdb.kugi.kyoto-u.ac.jp/) provides a quick-look *Dst* in near-real time [*Kamei and Sugiura*, 1996].

Development of geomagnetic storm models has been complicated by evidence that substorms were essential to *Dst* evolution [e.g., *Akasofu*, 1981; *Kamide and Allen*, 1997; *McPherron*, 1997]. However, it seems possible to proceed under the assumption that while storms and substorms are physically coupled, they are parallel and/or symbiotic, not sequential processes, thus explaining the success of algorithms that predict *Dst* directly from solar wind input. In the United States, the National Space Weather Program has developed a Strategic Plan (1995) and an Implementation Plan (1997), which emphasize understanding and predicting of geomagnetic disturbances.

The largest geomagnetic storms arise from Earth passage of the structures now associated with the interplanetary manifestations of coronal mass ejections [*Tsurutani et al.*, 1988; *Wilson*, 1990; *Gosling et al.*, 1991]. Improved understanding of flux-rope-type features of coronal mass ejections are leading to predictive schemes for storm development [*Chen et al.*, 1996; 1997].

3.1. Prediction of Magnetic Storms From Solar Wind Variables

The solar wind is the driver for both forms of geomagnetic activity, viz., storms and substorms. In the case of storms, the relationship between solar wind-induced dawn-dusk electric fields $E_w = VB_s$ and *Dst* was first studied by *Burton et al.* [1975], showing a strong correlation. The most widely used technique for such empirical studies has been the linear prediction filter [e.g., *Iyemori et al.*, 1979; *Clauer*, 1986]. This technique uses the past input-output data to obtain an impulse response filter of the system, which is then used to characterize the degree to which the system is linearly driven by the input. Such a study of substorms using the solar wind VB_s as the input and *AL* as the output found that only 40% of the variance of the *AL* index is predictable [*Bargatze et al.*, 1985], implying the important role of internal processes such as loading-unloading in magnetospheric dynamics. In the case of magnetic storms, the prediction filters for *Dst* obtained from the solar wind dynamic pressure and the electric field for a 52 hour data set [*Fay et al.*, 1986] as input showed that 70% of the *Dst* variance is predictable. Thus these studies indicated a higher degree driving of the ring current by the solar wind than the auroral electrojets.

The linear prediction filter studies of the solar wind-magnetosphere coupling indicate the role of nonlinear processes. Extensive studies of substorms using *AE*, *AL* and solar wind VB_z time series have given accumulated evidence that the magnetosphere behaves as a nonlinear dynamical system which can be described by a small number of variables. These studies of the low-dimensional nature of substorms and their predictability have recently been reviewed [*Sharma*, 1995; *Klimas et al.*, 1996]. In the case of magnetic storms the linear prediction filters have provided weaker evidence for nonlinear processes. However, the *Dst* decay time τ has been found to depend nonlinearly on the magnitude of magnetic storms [*Gonzalez et al.*, 1989].

The OMNI database is a convenient and widely used source for studying intense magnetic storms: see the http://nssdc.gsfc.nasa.gov/omniweb/ow/html Web site. In fact, for the period 1964-1990 this database contains 140 intense storms with *Dst* values below –100 nT. The solar wind data however are not available for most of these intense storms. Defining a storm interval that begins 10 hours before the *Dst* goes down to –50 nT during the main phase, and ends another 10 hours after the *Dst* returns to the same value in the recovery phase, the OMNI database contains only 14 storms with simultaneous measurements of the solar wind variables. Further, in these cases the *Dst* was required to be persistently above –50 nT during the two 10-hour intervals [*Valdivia et al.*, 1996]. Variations of the solar wind ram pressure nm_+V^2, where n and V are the solar wind density and speed, respectively, and m_+ is the proton mass, produce changes in the magnetopause currents, which in turn, affects significantly the magnetic field measured at low latitudes. A simple technique [*Burton et al.*, 1975; *Gonzalez et al.*, 1989] is used to subtract this effect to obtain the pressure corrected *Dst* (denoted on *Dst**) as

$$Dst^* = Dst - b\,(nm_+V^2)^{1/2} + c.$$

The values of the constants computed for this dataset are $c = 22$ nT and $b = 0.31$ nT/(eV cm^{-3})$^{1/2}$ = 10.5 nT/(nPa)$^{1/2}$, and are slightly different from the earlier values. The pressure corrected *Dst* is a better representation of the changes in the ring current during storms and should be used when the solar wind data are available.

In the *Burton et al.* [1975] model, the time development of *Dst* is modeled in terms of an input or injection function $Q(t)$ and a recovery with a characteristic time scale τ, so that

$$dDst^*(t)/dt = Q(t) - Dst^*(t)/\tau.$$

The input function $Q(t)$ is widely taken to be the solar wind induced electric field in such models, but other forms also have been used [see *Gonzalez et al.*, 1994]. This model can be generalized to include the nonlinearity in the evolution of *Dst* by considering a generalized form of the right hand side. Taking the normalized electric field $E_w = VB_s\,\sigma_{Ew}/\sigma_{Dst}$, where σ_{Dst} = 44 nT and σ_{Ew} = 3.7 mV/m, a predictor-corrector integration scheme yields an ordinary differential equation (ODE):

$$dDst^*(t)/dt = -0.08\,Dst^*(t)\,[1 - 0.0012\,Dst^*(t)] + 0.26\,E_w(t)$$

The decay time τ is given by the inverse of the coefficient of *Dst** and has a value of $\tau \sim 12.5$ hours, which is consistent with

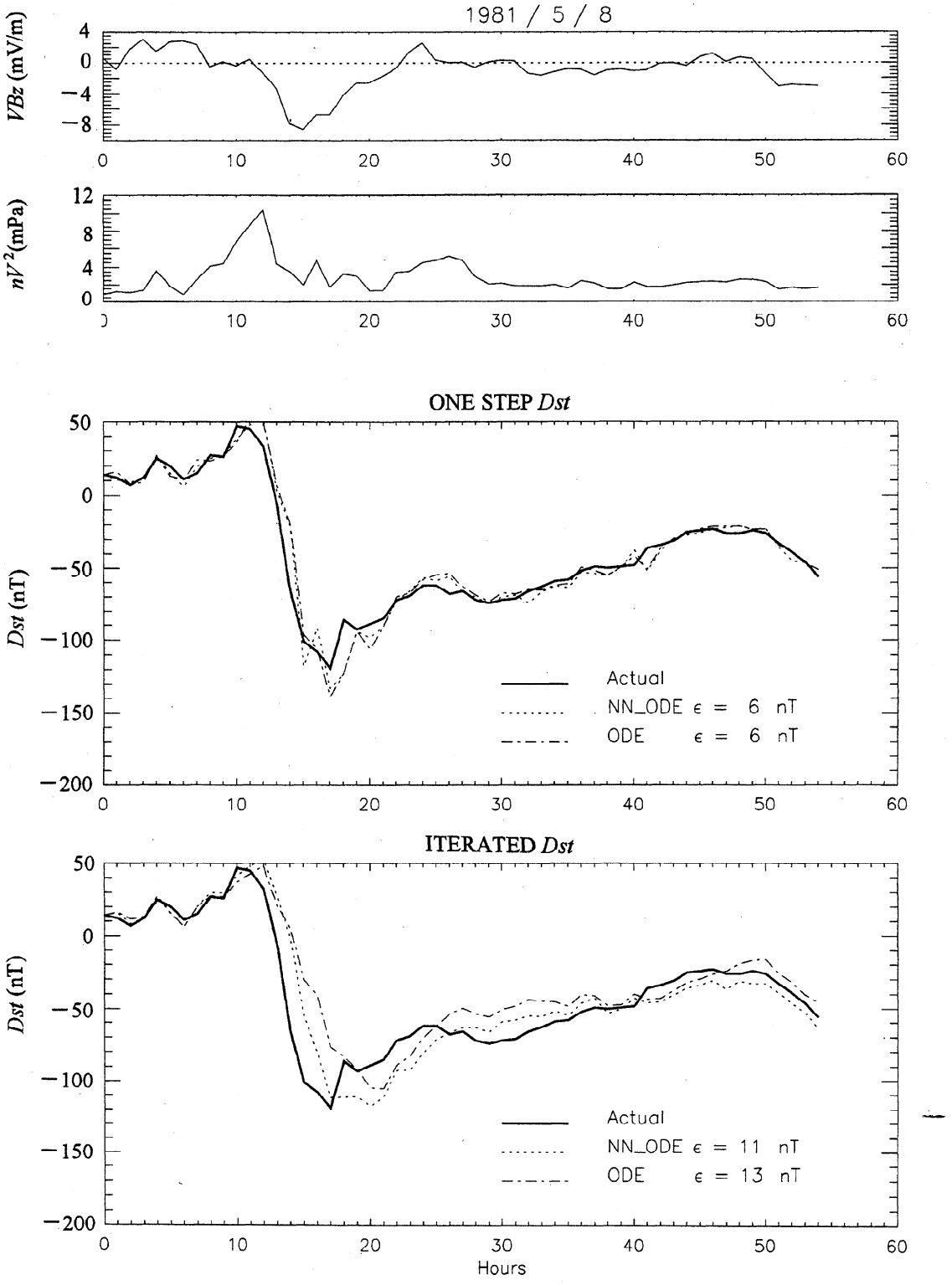

Figure 8. The prediction for the magnetic storm of May 8, 1981, using local linear (nearest neighbor) technique. The top two panels show the solar wind VB_z and the dynamic pressure. The one step and iterated predictions of the *Dst* are compared with the predictions in the bottom two panels. The *Dst* predicted by the nearest neighbor technique in which the functional form is taken to be an ordinary differential equation is given by the dotted line (marked NN_ODE). The predictions given by an ordinary differential equation of the *Burton et al.* [1975] form with *Dst* dependent decay rate, are given by the dotted-dashed lines (marked ODE). The phase space was reconstructed using 13 out of the 14 selected storms in the OMNI database and then predicted for the 14th storm and is thus out of sample.

earlier studies [see *Gonzalez et al.*, 1994]. A *Dst** dependent decay time can be defined as

$$\tau = \tau_0/(1 - 0.0012\ Dst^*)$$

with τ_0 = 12.5 hours. Thus, for $Dst^* \le -100$ nT, the variations of τ due to the nonlinear dependence are significant: more intense storms have shorter recovery time scales.

The above ordinary differential equation (ODE) for the evolution of *Dst* can be used to predict the time development of storms from the solar wind induced electric field E_w in two ways. In the first method, the observed $Dst\,(t)$ and $E_w\,(t)$ at time t are used to predict the *Dst* at the next time step t+1. To predict the *Dst* at t+2, the observed or actual values of *Dst* and E_w at t+1 are used. These are one-step predictions in which the observed values are used to predict the next values. The one-step predictions for the magnetic storm of May 8, 1981, are shown by the dotted-dashed line marked ODE in the middle panel of Figure 8. In the second method, multistep or iterated predictions are obtained by using the actual *Dst* and E_w at time t to predict $Dst\,(t+1)$ at time t+1 and then using this predicted *Dst* and actual value of E_w to obtain the next value, and so on. The iterated predictions for 55 hours for the May 8, 1981 magnetic storm are shown by the dotted-dashed line marked ODE in the bottom panel of Figure 8. The input to the prediction model needed to predict *Dst* in the next time step is the actual *Dst* and E_w in the case of one-step method. On the other hand, in the iterated method the actual *Dst* and E_w are used to start the predictions, and subsequently the observed *Dst* and actual E_w are used to obtain further predictions. Thus, in the one-step method the *Dst* values are updated before every prediction, whereas in the multistep method the predicted *Dst* and actual E_w values are used to obtain the predictions. Consequently the multistep prediction suffers from accumulated errors in *Dst* and the one-step method yields better predictions.

The inadequacy of a single decay time in modeling the time evolution of *Dst* has been pointed out in many linear models. *Feldstein et al.* [1984] obtained a decay time of 5.8 hours for $Dst < -55$ nT and 8.3 hr for $Dst > -55$ nT. Using the solar wind input $\varepsilon = VB^2 \sin^4(\theta/2)\ l_0^2$ [*Perreault and Akasofu*, 1978], where B is the IMF magnitude, θ is the colatitude of the IMF projected on the *y-z* plane (GSM) and l_0 is a constant (= 7 R_E), *Akasofu* [1981] obtained decay times of 1 hour for $\varepsilon > 5 \times 10^{18}$ erg s^{-1} and 20 hours for $\varepsilon < 5 \times 10^{18}$ erg s^{-1}. A superposition of two decay times for an optimized coupling function given by

$$F_0 = B_s^{1.09}\ V^{2.06}\ D^{0.38}$$

where D is the solar wind proton density, was studied by *Murayama* [1986] and *Maezawa and Murayama* [1986].

3.2. Input-Output Phase Space Reconstruction

Considering the solar wind-magnetosphere interaction to be a natural input-output system, its dynamical features can be reconstructed on the storm time scale by using the method of time delay embedding [*Packard et al.*, 1980; *Takens*, 1981] adapted to input-output systems [*Casdagli*, 1992]. These techniques have recently been reviewed [*Detman and Vassiliadis*, 1997]. The dusk-to-dawn electric field $E_w = VB_s$ is chosen as the input variable and the *Dst* as the output. The reconstructed phase space is represented by the state vector

$$\boldsymbol{X}(t) = [Dst^*(t), \ldots, Dst^*(t - (m_{\text{out}} - 1)\tau_{\text{out}}; E_w(t), \ldots, E_w(t - (m_{\text{in}} - 1)\tau_{\text{in}}].$$

The parameter m_{in} is the number of dimensions (embedding dimension) chosen to represent the input system, and similarly m_{out} is the embedding dimension of the output system. A time delay τ is normally chosen to capture the dynamical features of the system. Since the data in the NGDC database are 1-hour averaged the time delays τ_{in} and τ_{out} are taken to be unity. These techniques have been used extensively in the study of magnetospheric dynamics, reconstructed from the *AE* and *AL* indices and the IMF data (see reviews by *Sharma* [1995] and *Klimas et al.* [1996]). The local-linear model [*Farmer and Sidorowich*, 1987], which is based on the local characteristics of the reconstructed phase space, has been used to predict substorm activity using an input-output technique. The input can be the solar wind parameters in general, but mainly the interplanetary convection electric field VB_s is used, and the auroral electrojet index *AL* or *AE* is the output [*Price et al.*, 1994; *Vassiliadis et al.*, 1995]. In the case of magnetic storms, these techniques have yielded good predictions of *Dst** for given solar wind input [*Valdivia et al.*, 1996]. In this technique, the *Dst** value at the next time interval $Dst^*(t+1)$ is expressed as

$$Dst^*(t+1) = F[\boldsymbol{X}(t)]$$

where the functional F of the state vector $\boldsymbol{X}(t)$ is obtained from the dynamical features of the reconstructed phase space. The local value of F is obtained by a Taylor expansion around $\boldsymbol{X}(t)$ and the coefficients computed by a fitting procedure using the evolution of the nearest neighbors of $\boldsymbol{X}(t)$. When the Taylor expansion is limited to the linear term this yields a local linear technique.

The local linear technique can be used to make one-step and iterated predictions. One-step predictions use the known $Dst^*(t)$ and $E_w(t)$ at time t to obtain the predicted $Dst^*(t+1)$ at the next time step t+1. Iterated predictions starting at time t+1 are made by using $Dst^*(t)$ and $E_w(t)$ at time t, and E_w at the subsequent time steps, t+1, t+2, t+3, etc. The predicted $Dst^*(t+1)$ and $E_w(t+1)$ are used to obtain $Dst^*(t+2)$ at the next time step, and so on. The case of the magnetic storm of May 8, 1981 is shown in Figure 8. The solar wind input VB_z, in the top panel, has the characteristic strong negative excursion lasting about 10 hours in the main phase followed by another weak negative excursion. The solar wind dynamic pressure, shown in the second panel from the top, is used to obtain the pressure corrected *Dst**, shown by the solid lines in the bottom two panels. The predictions are obtained by using the nearest neighbor technique with the coupling expressed as an ordinary differential equation, and are shown by the dotted line (marked NN_ODE) in the second panel from the bottom. In this one step prediction the predicted *Dst* value is not used for the next prediction. The correlation between the actual and predicted *Dst* values computed over the 55-hour period is 0.96 and the mean absolute error is ~ 6 nT. The iterated prediction is shown in the bottom panel of Figure 8. The correlation is lower at 0.81 with the error being higher at 11 nT. Out of the 14 storms chosen from the OMNI database by using the criteria described in the previous section, 13 were used to reconstruct the phase space and the prediction made for the remaining one. The local linear Taylor expansion for the functional F, which is actually a local filter, can capture the global structure of the system by adjusting itself to different conditions of the ring current and the solar wind, yielding good predictions of the *Dst* index.

3.3. Prediction of Geomagnetic Activity Using Neural Networks

Neural network techniques are input-output models and are efficient in capturing the linear as well as nonlinear processes. This technique has recently been used to model and predict the

solar wind-magnetosphere coupling during storms and substorms (see review by *Lundstedt* [1997]). In the case of substorms, the *Bargatze et al.* [1985] data set was analyzed using neural networks for the relationship between VB_s and *AL*. They obtained prediction efficiencies of 76% for a nonlinear feed-forward network as well as a linear stochastic model [*Hernandez et al.*, 1993]. A study of different coupling functions for better prediction of substorms has given a prediction of 71% of the variance of the *AE* index for the best coupling function, namely, $p^{1/2}V^2B_s$. The directly driven model of *Goertz et al.* [1993] yields a very high correlation coefficient of 0.92 between VB_s and *AE*, higher than the neural network or local-linear models discussed above. However, problems related to the filtering of the data, possible data bias and also the limited dataset used in their model have been noted [*McPherron and Rostoker*, 1993].

Magnetic storm prediction studies using neural networks have been made for different coupling functions using the OMNI database for the period 1963-1992 [*Wu and Lundstedt*, 1996, 1997]. For 1 hour predictions, the optimum function, $p^{1/2}VB_s$ yields a root mean square error of 17 nT and a slightly higher error for VB_S. If a combination of the solar wind variables is used instead of a single coupling function, the error is reduced to 14 nT. The local linear techniques seem to yield slightly better 1 hr predictions, although it is difficult to compare the results from these different techniques in view of the different data sets, lengths of data, lengths of the predicted periods, etc. One notable difference between these two very similar techniques is the ability of the local linear technique to make iterated prediction, yielding long term predictions as shown in the bottom panel of Figure 8. Suitable modifications of Elman recurrent neural networks may yield techniques that can be used to describe temporal behavior, thus making iterated predictions possible [*Lundstedt*, 1997]. Neural network techniques are used to routinely predict *Dst* for input into the MSFM [*Freeman et al.*, 1994; *Costello*, 1996].

3.4. Prediction of *Dst* From *AL*

The strong correlation between intense substorms and the main phase of magnetic storms indicates a cause-effect relationship. The scenario of a sequence of substorm injections leading to a magnetic storm is attractive from physical considerations and has observational support [*Gonzalez et al.*, 1994]. The simplest picture is to consider a magnetic storm being driven by a sequence of substorms, and such a model that uses the *AL* as the driver reproduces the *Dst* index quite well [*Kamide and Fukushima*, 1971]. The differences in the *AE-Dst* relationship during moderately disturbed geomagnetic conditions and during storms were studied by *Akasofu* [1981]. Using high-resolution (2.5 min) data, *McPherron* [1997] used prediction filters to predict *Dst* and *AL* from VB_s and found that the prediction residuals of the two indices are completely uncorrelated. This indicates that the effect of the particle injections and subsequent energization during the expansive phase of substorms are undetectable in *Dst*.

The input-output phase space reconstruction technique is suitable for studying such cause-effect relationships. Using the 5-min average *AL* data for January 1 to June 30, 1996, as the input, the *Dst* index for March 9, 1979 storm is predicted using the local linear technique, as shown in Figure 9. The top panel shows the *AL* index, the middle panel shows the solar wind dynamic pressure, and the bottom panel compares the actual and predicted *Dst*. The dashed curve is the prediction by the local linear technique, the dotted curve is a simple relationship similar to that of *Burton et al.* [1975]. Both the predictions agree quite well, and the local linear predictions capture more details of the *Dst* variations.

Alternatively, the *AL-Dst* relationship can be expressed as

$$Dst\,(t+1) = \alpha \int_0^{\tau} dx\, e^{-\beta x} AL\,(t-x)$$

where the constants α, β, and τ are determined from the data. The 5-min-averaged *AL-Dst* data for January 1 to June 1, 1979, is used to optimize the coefficients in this relationship and yield the values $\alpha = 0.003$, $\beta = 0.001$ and $\tau = 8$ hours. With these values the prediction of the storm of March 9, 1979, from the *AL* is shown in Figure 10. The agreement between the actual and the predicted *Dst*, particularly in the neighborhood of the storm peak, is found to be very good.

4. Particle Injection

Geomagnetic storms have very dramatic effects when viewed in geosynchronous energetic particle measurements. This is illustrated in Figure 11 that shows a rather typical storm, which began on November 3, 1993. This storm was chosen for study by the GEM and CEDAR communities and has come to be known as the National Space Weather storm [*Knipp and Emery*, 1997]. It is illustrative both because it shows much of the behavior that is expected in geosynchronous energetic particle measurements and because it illustrates some of the things that are still not well understood about the relationship between geosynchronous energetic particle observations and the development of geomagnetic storms.

Figure 11 shows geosynchronous energetic particle data and the *Dst* index for the 36-hour interval from 1200 UT on November 3 to 0000 UT on November 5. The top two panels show proton and electron data from satellite 1984-129, the next two panels show proton and electron data from satellite 1989-046, and the bottom panel shows the 1-hour *Dst* index. Satellites 1984-129 and 1989-046 were two of the five Los Alamos geosynchronous satellites carrying Los Alamos particle detectors that were operating at this time. Satellite 1984-129 was located at 8 deg. west longitude and therefore passed midnight local time at approximately 2330 UT each day. Those times are marked with solid vertical lines on the plots. Satellite 1989-046 was nearly on the opposite side of the Earth at 165 deg east longitude which brought it past midnight at about 1100 UT as is also marked on the plots.

As with most storms, energetic particle injections are observed on the nightside of the Earth throughout the main phase of the storm. The geosynchronous energetic particle fluxes have a large dynamic range during storms. When the magnetic field becomes highly stretched the satellites become magnetically connected to the more distant plasma sheet where energetic particle fluxes are lower and a characteristic dropout of particles is generally observed on the nightside. When the field dipolarizes the fluxes not only return to their undisturbed levels but are enhanced indicating energization of the distribution. Storms are characterized by frequent oscillations of the particle fluxes, by extreme and prolonged periods of taillike fields, and by numerous and highly structured particle injections at geosynchronous orbit.

The injection activity in this interval began in close association with the negative dip in *Dst* and continued throughout the next 24 hours. The intensity of the injections is strongly dependent on the location of the satellites and the direction of the particle drift. 1984-129 saw the most intense electron injections from 0000 to 0800 UT when it was postmidnight and could easily observe the electrons which were injected near midnight and drifted east. Likewise 1989-046 observed the strongest electron injections when it was near or postmidnight (0800 to 1800 UT). Since ions drift west the situation is opposite: 1989-046 observed the strongest ion injections in the first half of the day when it was premidnight and 1984-129 observed the strongest ion injections in the second half of the day when it was located premidnight.

Now let us consider these observations in a little more detail. At the beginning of the interval shown the IMF B_z was northward and magnetospheric conditions had been extremely quiet for nearly 2 days. At approximately 1720 UT a sudden commencement was recorded as the magnetosphere was

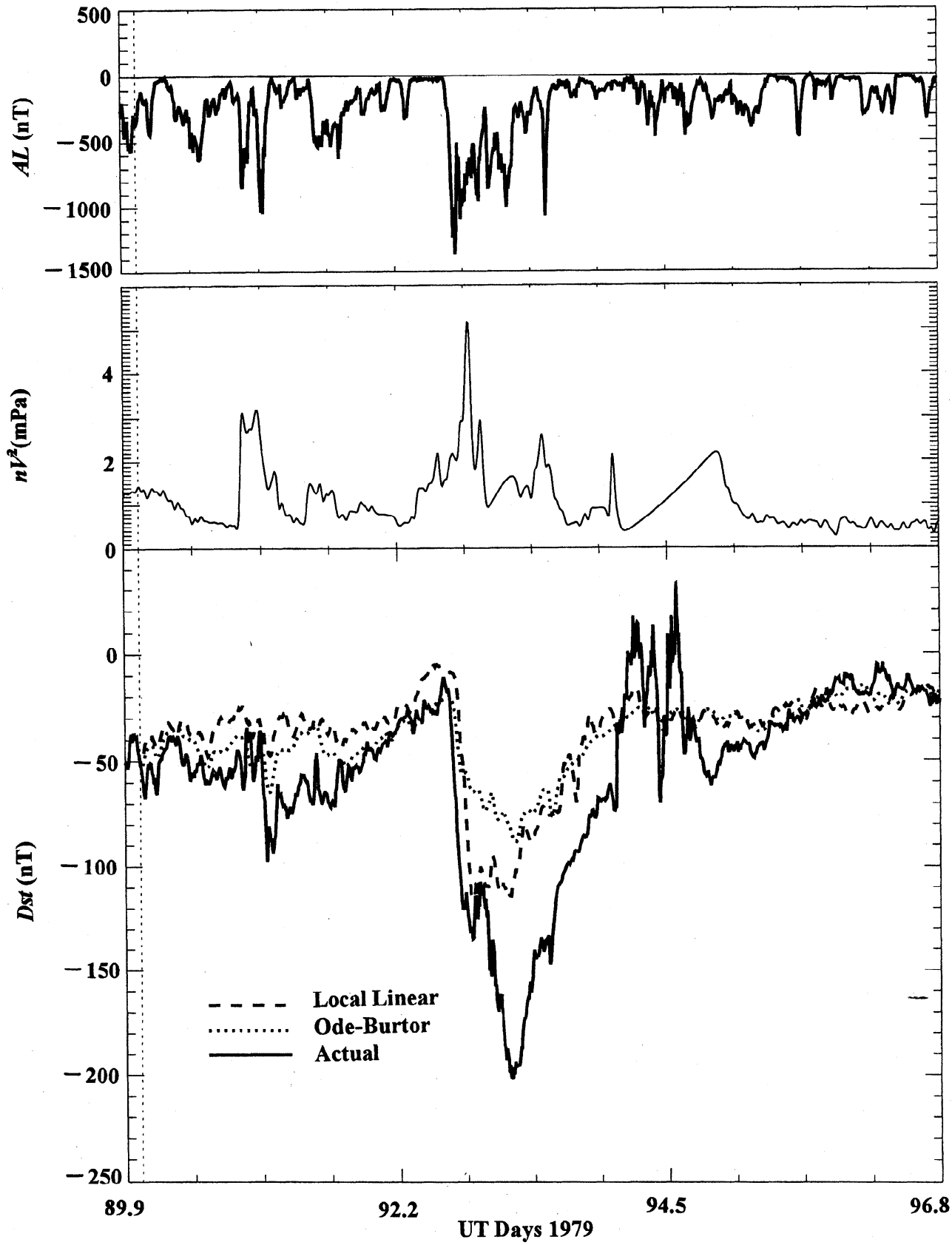

Figure 9. The *Dst* for the storm of March 9, 1979, predicted from the *AL* as the input in the local linear technique: (top) *AL* index, (middle) solar wind dynamic pressure, (bottom) actual *Dst* (solid line), *Dst* predicted from *AL* using local linear technique (dashed line) deviates from the actual *Dst* (dotted line) and *Dst* predicted from an ordinary differential equation of the *Burton et al.* [1975] form. Both the *AL* and *Dst* indices are 5 min averaged.

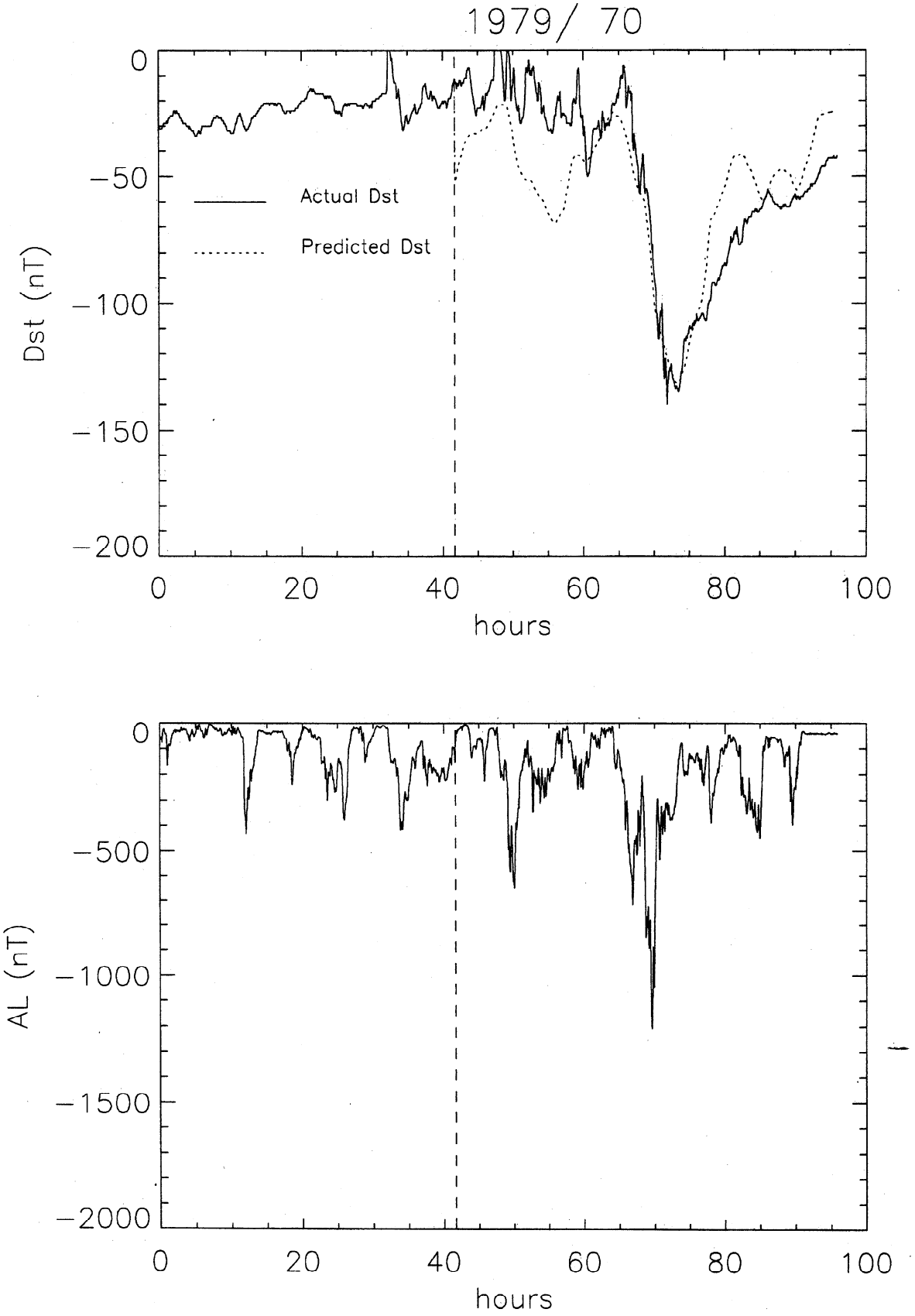

Figure 10. The *Dst* (top panel, dotted line) for the storm of March 9, 1979, obtained from the optimized fit tracks the actual *Dst* (the continuous line) well during the main phase.

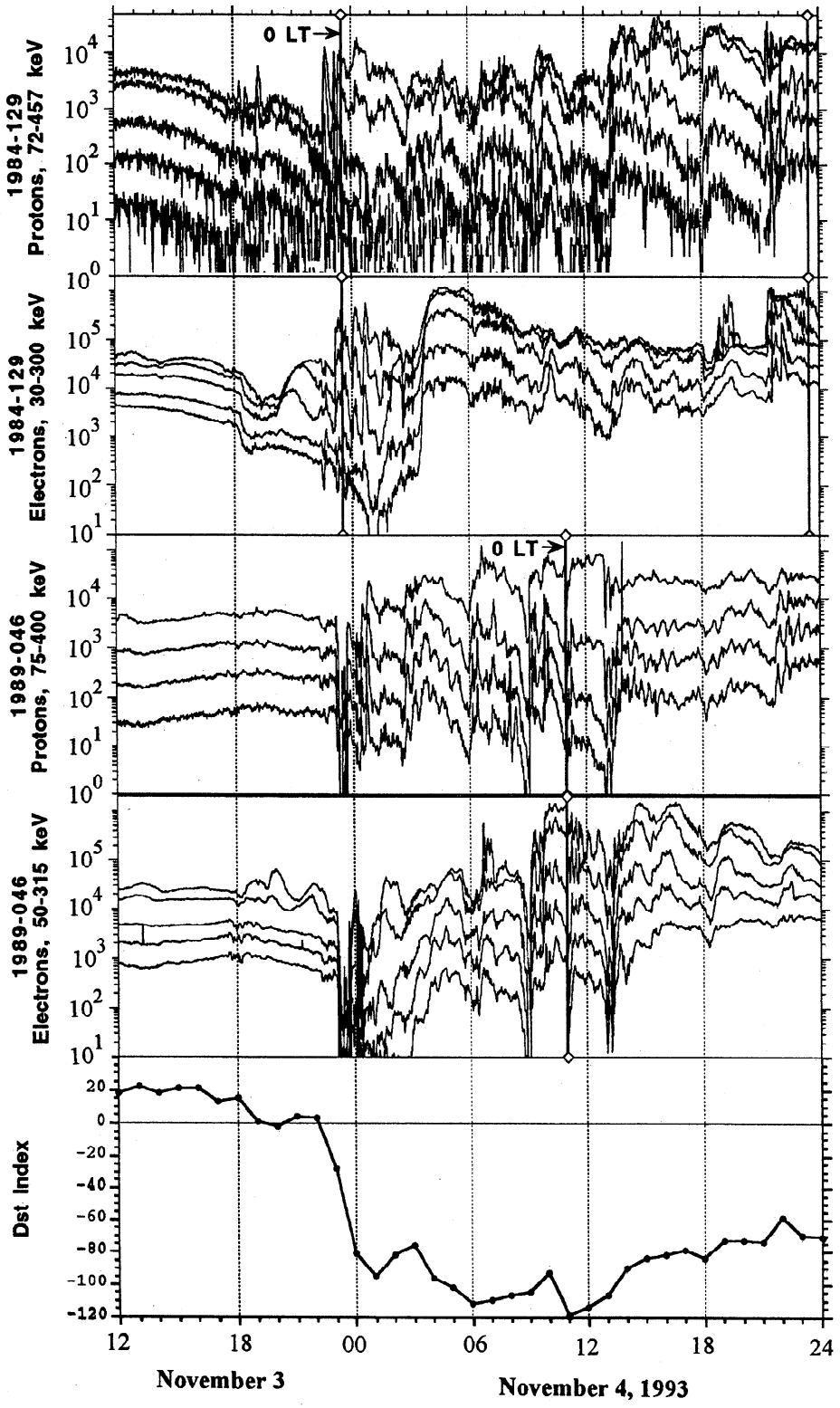

Figure 11. The response of geosynchronous energetic particles to the November 3-5, 1993, geomagnetic storm known as the "National Space Weather Event." The figure shows proton and electron fluxes from two geosynchronous satellites along with the *Dst* index for this period. Very strong injections of energetic particles are observed. However, a direct, quantitative relationship between geosynchronous injections and the development of *Dst* is difficult to establish.

disturbed by an interplanetary shock associated with a high-speed solar wind stream originating in a solar coronal hole. The IMF B_z did not become significantly southward until about 2200 UT and the first indications of energetic particle injections were observed in the ions at spacecraft 1984-129 at about 2230 UT. Satellite 1984-129 did not record an electron injection at that time which indicates that the injection region was restricted to locations east of the satellite (e.g., east of 2100 LT). A dispersionless injection of both ions and electrons was then observed at 2306 UT (2236 LT). At approximately the same time spacecraft 1989-046,

located near noon, observed a dropout of energetic particles when the satellite crossed the magnetopause indicating that the dayside magnetosphere was strongly compressed. The close association of the nightside injection and the dayside dropout may be coincidental or it may indicate that both were produced by an enhancement in the solar wind dynamic pressure.

The observations of the onset of this storm again illustrate the importance of southward IMF B_z to the coupling of energy from the solar wind to the magnetosphere, to the energization and injection of particles at geosynchronous orbit, and to the development of the storm time ring current. One interpretation of these observations is that the injections are caused by substorms and that a rapid sequence of substorm injections energize a large number of particles, particularly ions, and transport them to the inner magnetosphere where they form the storm time ring current and produce the classic signature seen in the *Dst* index. Clearly, there is some truth to this picture but is it the entire explanation?

There is some controversy over the application of the term "substorm" to the injection signatures seen during storms. A substorm is generally thought of as being, at least in some regards, a global and coherent process with a growth phase, dipolarization, and energization of particles. During storms the changes in the magnetic field and injections of particles are so rapid that it becomes difficult, if not impossible, to identify individual substorms. Indeed observations from two satellites that are both on the nightside often show very little coherence and can frequently show growth phase and injection signatures simultaneously at locations separated by only a few hours of local time.

A more significant problem with identifying the injections seen at geosynchronous orbit with the development of *Dst* is the lack of correlation between the value of *Dst* and injection activity at geosynchronous orbit. In this storm, as with many others, *Dst* dropped to nearly –100 nT in 3 hours. However, if one were to look only at the first 3 hours of geosynchronous energetic particle data, they would not look particularly unusual. Many intervals of substorm activity produce similarly intense injections of ions and electrons without having much effect on *Dst*. A related question is why intense periods of substorm activity during the recovery phase often seem to have little effect on the recovery of *Dst*. The sequence of injections seen shortly after 2100 UT near the end of the interval plotted in Figure 11 is one example.

The minimum in *Dst* for this storm was –119 nT observed at 1100 UT on November 4. However, the injection activity at geosynchronous orbit did not appreciably diminish until after 1800 UT. We note in particular the ion injection activity observed after 1100 UT by spacecraft 1984-129 which was in a good location to observe ion injections at that time. In Figure 9 the motion of the spacecraft makes it somewhat difficult to separate temporal effects from the dependence on the local time of the satellites. However, when data from all five satellites are plotted on top of one another, there is no obvious peak in injection activity prior to 1100 UT or diminishing of activity when *Dst* begins to recover. It is also notable that the spectrum of both ions and electrons is noticeably harder (as indicated by a smaller ratio of low- to high-energy fluxes) at 0000 UT on November 5 than it was at the peak in *Dst* 13 hours earlier.

When examining the storm-substorm relationship from the perspective of geosynchronous orbit, it is important to keep in mind that geosynchronous orbit is at a fixed radial distance and is not a fixed magnetospheric regime. Normally, geosynchronous orbit lies near the outer edge of the stable trapping region for particles with energies of tens to hundreds of keV. During substorms the inductive electric field can convect particles from the tail which previously did not have access to geosynchronous orbit.

The sudden reduction of that electric field leaves those particles on trapped drift orbits. During storms, however, the global convective electric field may frequently be strong enough to move the stable trapping boundary inward of geosynchronous orbit. Fluctuations of the stormtime electric field, both substorm expansion-related and directly driven, would then be expected to energize and trap particles well inside geosynchronous orbit.

Whether the injections of energetic particles seen at geosynchronous orbit during storms can be identified with substorms or not and whether they are the source population for the storm time ring current, it is clear that they are in important part of the overall process that we identify as a geomagnetic storm. Multisatellite analysis has shown that during an isolated substorm the injection front can propagate from geosynchronous orbit in to approximately $L = 4$ [*Reeves et al.*, 1996]. While simultaneous measurements at different L shells during storms are much more difficult to interpret considerable effort along those lines is currently underway. This effort is aided considerably by energetic neutral atom (ENA) imaging, which has recently been able to provide global images of the ring current injection process that can be combined with in situ observations to investigate the storm-substorm relationship in unprecedented detail [*Henderson et al.*, 1997].

5. Ionospheric Particles in the Ring Current

The role of ionospheric particles in the ring current evolution during storms became evident only after the Active Magnetospheric Particle Tracer Explorers (AMPTE) mission [*Krimigis et al.*, 1982]. Previously the composition of the bulk ring current (i.e., within the energy range 20-300 keV) was unknown [e.g., *Williams*, 1983]. The charge energy mass (CHEM) spectrometer on board AMPTE/CCE was the first experiment to investigate the near-Earth magnetotail with multispecies ion measurements extending in the higher-energy (>20 keV) range [see *Glockler and Hamilton*, 1987].

The AMPTE lifetime coincided with the solar minimum, and only one great storm was observed. The great storm of February 1986 was studied in detail by *Hamilton et al.* [1988]. It was shown that the ionospheric-origin ions dominated the ring current near the storm's maximum phase. O^+ alone contributed 47% of the total ion energy density compared with 36% contributed by H^+. *Hamilton et al.* [1988] estimated that 67-80% of the ring current density near the maximum of the storm was of ionospheric origin (since also a fraction of H^+ and He^+ is of ionospheric origin). Consequently, the authors suggested a major ionospheric ring current component near the maximum phase of great storms.

The next opportunity for multi species measurements in the inner magnetosphere was provided by the Magnetospheric Ion Composition Spectrometer (MICS) experiment [*Wilken et al.*, 1992b] on board CRRES: the CRRES mission coincided with solar maximum. Observations regarding the ring current composition of the great storm in March 1991 were first presented by *Wilken et al.* [1992a]. The spectra and pitch angle distributions gained by MICS showed that new particles of predominantly ionospheric origin entered the inner magnetosphere during the storm main phase. O^+ was the dominant ion species near the storm maximum phase. Its contribution to the total energy density in the L range 5 to 6 reached the extraordinary level of 75%.

Daglis [1997] studied the importance of the ionospheric ion component in the ring current during several storms observed by CRRES, showing that during the main phase of great storms, the abundance of ionospheric origin ions (O^+ in particular) in the inner magnetosphere is extraordinarily high. Five storms during the period January to July 1991 were presented, with the peak $|Dst|$ ranging from 80 to 300 nT. The outstanding storm feature manifested by the CRRES observations was the concurrent increase of $|Dst|$ and of O^+ (and, consequently, ionospheric) contribution to the total particle energy density. Furthermore, it

was manifested that O^+ is the dominant ion species during the main phase of large storms: see Figure 12.

Considering the domination of O^+ and taking into account that a fraction of H^+ is also of ionospheric origin, *Daglis* [1997] suggested that the cause of the intense ring current during large storms is terrestrial, although the energy source is unambiguously of solar origin. According to *Daglis* [1997], very intense ring currents responsible for very low *Dst* levels are only created when the ionospheric response to the solar wind - magnetosphere coupling is of sufficient strength and temporal extent. However, the question if the ionospheric response is a prerequisite for very strong ring currents can only be addressed through a larger database of storm observations with composition measurements of the bulk ring current. It is noteworthy that preliminary modeling of the effects of outflowing O^+ on storm evolution [*Wodnicka*, 1991] has shown that an increase of injected O^+ ions with small initial pitch angles would increase the magnetic storm amplitude; low radial injection distances and higher initial energies would enhance the effect.

The CRRES (and previous AMPTE) observations have shown that the enhanced magnetosphere-ionosphere coupling, in form of ion feeding of the inner plasma sheet, provides the additional new population associated with the storm main phase. However, in order to fully assess the role of magnetosphere-ionosphere coupling in magnetic storm evolution, one does not only need compositional measurements in the inner magnetosphere but also complete information on the solar and interplanetary conditions preceding and accompanying large storms. In this way it will be possible to investigate if similar solar wind conditions lead to similar-size storms independently of the extent of ionospheric outflow.

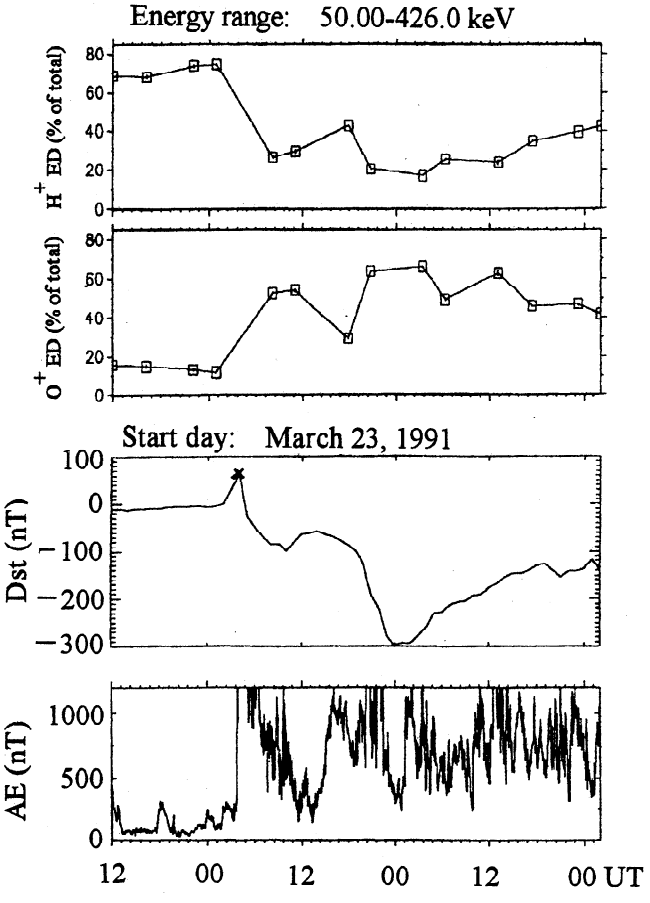

Figure 12. Time profile of the contribution of H^+ and O^+ to the total energy density of energetic ion population in the outer ring current during the great magnetic storm of March 1991 (top two panels), as well as the *Dst* index (third panel) and the *AE* index (bottom panel). The outstanding feature is the concurrent increase of the *Dst* magnitude and of the O^+ contribution to the total energy density. At storm maximum, when *Dst* reached −300 nT, O^+ became the dominant ion species, contributing more than 66% of the total ion energy density in the ring current.

The increased relative abundance of ionospheric O^+ ions in the inner magnetosphere during storms, besides influencing the ring current enhancement, influences the decay rate of the ring current, since the charge exchange lifetime of O^+ is considerably shorter than the H^+ lifetime for ring current energies ($\geq$ 40 keV) [see *Smith and Bewtra*, 1978; *Kozyra et al.*, 1997]. This implies that O^+-dominated ring current will decay faster, at least initially. Such a fast initial ring current decay, associated with a large O^+ component during the storm main phase, has been indeed observed in the February 1986 storm [*Hamilton et al.*, 1988]. The same trend was seen in the storms of July 9 and March 24, 1991 [*Daglis*, 1997], where the initially fast recovery of *Dst* is concurrent with an initially fast drop of the O^+ contribution to the total energy density.

The issue of the importance of substorm occurrence for the storm time ring current growth [*Kamide*, 1979, 1992] may be related to the connection of substorms with ionospheric outflow, since the ring current growth is concurrent with increased abundance of ionospheric origin ions in the inner equatorial magnetosphere. *Daglis et al.* [1992, 1994] showed, on the basis of a large set of substorm observations by AMPTE/CCE, the association of strong substorms (as observed during storms) and enhanced ionospheric ion abundance in the inner plasma sheet. A recent study of substorms observed by CRRES confirmed the AMPTE/CCE results [*Daglis et al*, 1996].

Further clues to this issue could be provided by studies of the processes of ionospheric ion extraction. Viking observations of ionospheric outflow and associated electric fields [*Lundin et al.*, 1987; *Hultqvist et al.*, 1988; *Lundin et al.*, 1990] prompted relevant modeling and simulation studies, which showed that outflowing ionospheric ions are accelerated very efficiently by low-frequency large-amplitude electric field fluctuations [*Lundin and Hultqvist*, 1989; *Hultqvist*, 1996]. Since such electric fields occur during intense auroral activity (G. Marklund, personal communication, 1997), it is expected that this type of acceleration of ionospheric ions at low altitudes operates during substorm expansion. Consequently, a higher abundance of ionospheric ions (O^+ in particular) in the inner magnetosphere is expected during substorm expansion, in accordance with the results of *Daglis et al.* [1994].

However, although several studies have shown that the outflow of ionospheric O^+ and the energy density of O^+ in the inner magnetosphere are closely correlated with auroral activity, the ring current grows more efficiently during the main phase of storms than during nonmain phase periods with the auroral electrojets having the same strength [*Gonzalez et al.*, 1994]. The answer to this paradox should be the persistence and long duration of enhanced auroral activity resulting in a prolonged ionospheric outflow during the storm main phase. A prolonged ionospheric outflow has been suggested by *Daglis and Axford* [1996] to account for the continuing rise in O^+ energy density in the inner plasma sheet, in contrast with the one-step rise of H^+ and He^{++} energy density during substorm expansion.

6. Tail Dynamics

The dynamics of the Earth's magnetotail is governed by unsteady convection and associated heating of the plasma, ranging from the high-speed flow bursts, which have time scales of some minutes, to the classical substorm with its 1-2 hour duration [see, e.g., *Baumjohann*, 1996]. Magnetic storms do, in

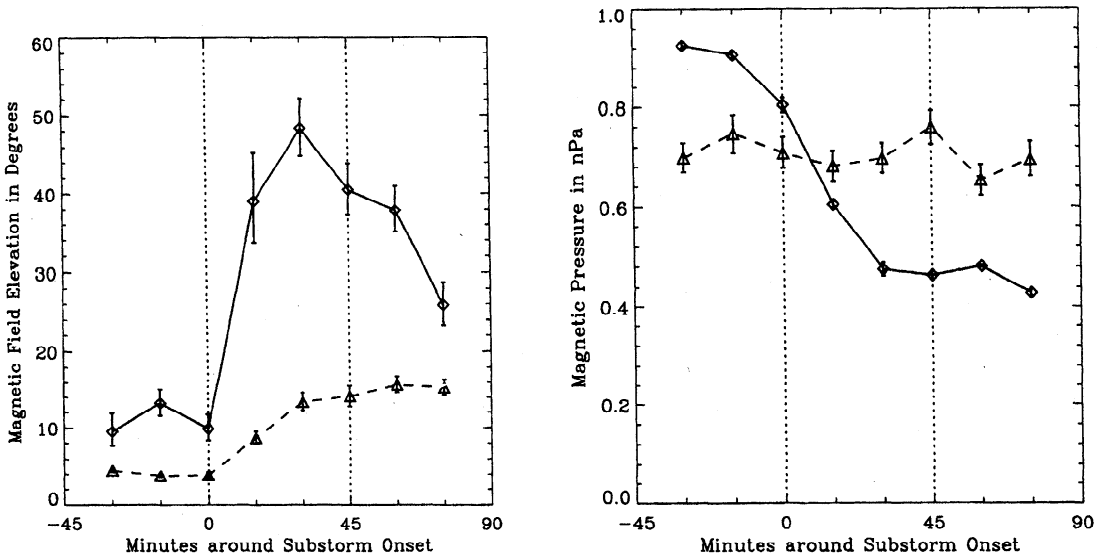

Figure 13. Superposed traces of the magnetic field elevation angle in the CPS (left-hand diagram) and of the magnetic pressure in the tail lobe (right-hand diagram) during storm time (solid traces) and nonstorm (dashed traces) substorms. The traces were constructed by averaging the measured values in 15-min bins with respect to substorm onset, separately for 7 substorms that occurred during the expansion phase of a magnetic storm and 35 substorms where the *Dst* index was above –25 nT. The dashed vertical lines mark substorm onset and the approximate start of the recovery phase.

principle, not change this behavior. They neither add a new way of transporting plasma inward nor do they add a new time scale. *Ho et al.* [1997] noted that deep tail plasma jetting is far more intense and frequent during storms than during nonstorm substorms. Magnetic storms, or more precisely, the steady southward IMF during their main phase, however, affects the way how substorms proceed. Furthermore, the immediate recurrence of several substorms produces a much hotter plasma sheet particle population.

6.1. Different Substorm Signatures

Baumjohann et al. [1996] conducted a superposed epoch analysis to study possible differences in the behavior of the near-Earth tail around substorm onsets that occurred during the main phase of a magnetic storm and those that were not accompanied by magnetic storm activity (*Dst* > –25 nT). Figure 13 shows that the average behavior of the near-Earth tail magnetic field at radial distances between 10 and 20 R_E is significantly different during the two types of substorms.

The difference between the two types of substorms becomes immediately clear in the development of the magnetic field elevation angle. During substorms that are not accompanied by magnetic storm activity, the magnetic field dipolarization appears to be very gradual, reaching its highest elevation angles only during the recovery phase. Moreover, the dipolarization is not very pronounced, with an average maximum elevation angle of only 15 deg. However, for substorms that occur during the storm main phase, the magnetic field in the CPS starts to become rather dipolar immediately after substorm onset and the maximum field elevation reaches nearly 50 deg.

The right-hand panel of Figure 13 shows the variation of the lobe magnetic pressure. Again, the difference between the two traces is most obvious. During nonstorm substorms, the lobe magnetic pressure does not change in any systematic way. However, the lobe magnetic pressure changes quite drastically during the expansion phase of storm time substorms. It starts from a somewhat higher level, but even more importantly, it drops to about half of its preonset value during the expansion phase.

For this type of substorm one can see a clear dipolarization of the tail magnetic field and the decrease in the strength of the lobe field, both of which are expected to be associated with the formation of a near-Earth neutral line tailward of the satellite during substorm onset and subsequent reconnection of closed plasma sheet field lines and open magnetic flux tubes intermediately stored in the tail lobes [e.g., *McPherron et al.*, 1973; *Hones*, 1984]. During the typical nonstorm substorm, we do also see a more dipolar field, but the dipolarization is weaker and maximizes only after the end of the expansion phase.

We may speculate that the somewhat different behavior of the IMF during storm time and nonstorm intervals results in quite different types of substorms, in line with arguments presented by *Cowley* [1992]. During the typical nonstorm substorm, the enhanced solar wind-magnetosphere coupling due to the southward component of the IMF leads to enhanced convection but the reconnection rate at the distant neutral line may be high enough to allow for the closure of all magnetic flux tubes that have been opened at the dayside magnetopause. Substorm expansion onset can then be the result of an instability developing due to the strongly enhanced current flow associated with the enhanced convection, either of the whole magnetosphere-ionosphere current circuit, as advocated by *Kan* [1988] or of the enhanced tail current around 6-8 R_E, as suggested by *Lui et al.* [1988]. The gradual increase of magnetic field elevation and earthward transport observed between 10 and 20 R_E is then the result of the tailward propagating collapse of the tail current that has been initiated much closer to the Earth [e.g., *Jacquey*, 1991; *Ohtani et al.*, 1992]. The collapse may or may not be accompanied by the tearing mode instability or magnetic reconnection. At any rate, it seems likely that the collapse occurs closer to the Earth and mainly closed magnetic field lines are involved in this process.

When the IMF has a strong southward component for a prolonged period of time, like during a magnetic storm, would the distant neutral line perhaps be unable to reconnect all the magnetic flux merged at the dayside magnetosphere. In this case there will be a surplus of open magnetic flux that is intermediately stored as magnetic field energy in the tail lobe and

then suddenly reconnected at a near-Earth neutral line. Since the formation of a new neutral line proceeds via the ion-tearing instability [*Schindler*, 1974], it may help that the central plasma sheet is already hotter, since more energetic ions will behave less adiabatic in the vicinity of the neutral sheet.

6.2. Recurrent Heating of the Plasma Sheet

Figure 14, again from the superposed epoch study of *Baumjohann et al.* [1996], shows the average ion temperature in the CPS, separately for storm time and nonstorm substorms. As in Figure 12, the traces are constructed by binning measurements taken by the IRM satellite in the CPS with respect to the particular onset and then averaging over all the samples in a particular 15-min bin. It clearly illustrates that the heating of the ion population in the CPS occurs during the substorm expansion phase. The temperature increase from substorm onset to the beginning of the recovery phase is about the same for both types of substorms, of the order of 2.5 MK, or roughly 2 keV. The difference, however, between storm time and nonstorm substorms lies in the average levels of the ion temperature before the onset, and thus also in the typical energy of the ion populations in the CPS during the expansion and recovery phases. In addition, the heating seems to occur more effectively during storm-time expansion phases, resulting in an average ion energy of 8 keV only 15-30 min after the onset of a storm time substorm, while the typical CPS ion has only 3-4 keV during the expansion phase of nonstorm substorms.

That the tail plasma is already quite energetic before the onset of the typical stormtime substorm must be a result of previous substorm activity, which is much more likely to occur during magnetic storm activity due to the sustained southward interplanetary magnetic field (IMF) and thus enhanced solar wind-magnetosphere coupling typical for the storm main phase. It may be that nonadiabatic heating [*Huang et al.*, 1992] is responsible for the larger energy gain of the plasma sheet ions during storm time periods. It is not unreasonable to argue that the tail plasma sheet plasma is already quite energetic before the onset of a storm time substorm. That is because there has already been considerable activity associated with the sustained southward IMF during which heating may have taken place both adiabatically and nonadiabatically. In fact, *Liu and Rostoker* [1995] have shown that it is possible for ions to achieve energy gains of up to some tens keV over several substorm cycles due to the nonadiabatic process of pitch angle scattering during the stretching and subsequent dipolarization of tail field lines during a substorm cycle. The process is an example of magnetic pumping first introduced by *Alfvén* [1949].

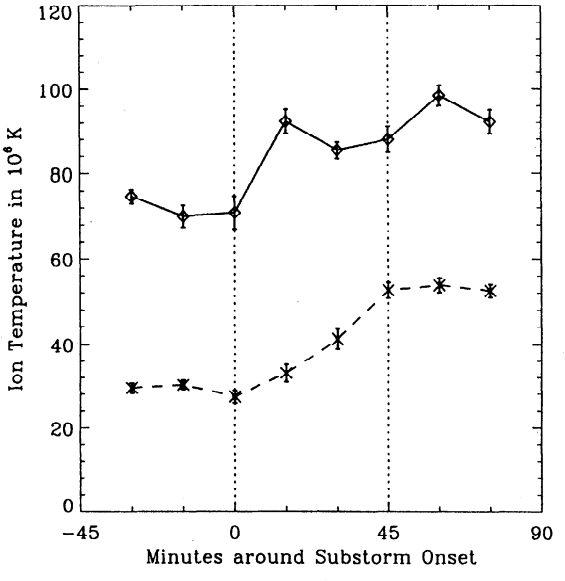

Figure 14. Average variation of the ion temperature in the CPS for substorms occurring during a storm main phase ($Dst < -25$ nT; solid line) and for nonstorm substorms ($Dst > -25$ nT; dashed line). The vertical error bars give the errors of the mean values. The dashed vertical lines mark substorm onset and the average start of the recovery phase.

6.3. Efficiency of Ring Current Injection

The *Dst* variation is the symmetric part of the magnetic disturbance caused by energetic particles encircling the Earth due to the combined effect of the gradient and curvature drift, in a near-dipolar field as well as the magnetization current. Hence what is needed to create a notable *Dst* variation, is to bring energetic particles from the tail close enough to the Earth so that they experience a gradient and curvature force strong enough to perform complete orbits around the Earth. Since the magnetic drift forces increase with increasing particle energy, more energetic particles will experience a stronger azimuthal drift for the same magnetic gradient and curvature. In addition, they will cause a larger *Dst* index, since the latter depends on the energy of the ring current particles.

Apparently, the much stronger dipolarization during the storm time substorms will bring the heated tail plasma closer to the Earth. Moreover, the plasma brought inward by storm-time substorm activity is more energetic and the more energetic particles will perform closed orbits at larger radial distances. Finally, once on closed orbits, the more energetic particles will cause a stronger field depression. This does not necessarily mean that no particles are injected into the symmetric ring current during nonstorm substorms, but at least the efficiency of energy injection into the ring current is much higher during the storm time substorms.

7. Discussion

7.1. Energy Budget Associated With Geomagnetic Storm Processes

Studies of energy input and dissipation in the magnetosphere associated with geomagnetic activity and related phenomena have been carried out for a long time: see, for example, *Hill* [1979], *Vasyliunas et al.* [1982], *Stern* [1984], *Weiss et al.* [1992], and *Gonzalez et al.* [1994, and references therein]. It is generally agreed that the power required to build up the storm time ring current and to supply the dissipation associated with various auroral and ionospheric manifestations of storms and substorms must be extracted ultimately from the kinetic energy of solar wind flow. Most of the dissipation processes (auroral particle acceleration, Joule heating in the ionosphere) as well as heating of plasma sheet and ring current particles by adiabatic compression and similar processes convert electromagnetic energy into mechanical energy of particle motion (either flow or thermal), whereas the energy supplied by the solar wind is initially all in mechanical form. Energy flow from the solar wind to the magnetosphere and ionosphere must therefore proceed in two steps: mechanical energy from the solar wind is converted to electromagnetic energy (and can be viewed as stored in the magnetic field primarily of the magnetotail), and this electromagnetic energy is converted to mechanical energy of particles in the plasma sheet, ring current, and ionosphere. Direct transfer of mechanical energy from the solar wind plasma in the magnetosheath into the adjacent magnetosphere is negligible on the global scale, consistent with the fact that the empirically estimated power input from the solar wind into the magnetosphere exceeds by an order of magnitude or more the

empirically estimated particle input from the solar wind multiplied by the solar wind kinetic energy per particle [*Hill*, 1974, 1979].

There is no general requirement that the two steps of the energy transfer must proceed at the same rate; on the contrary, various plausible scenarios can be constructed where the energy is first stored in the magnetotail and only subsequently, i.e., at a later time, released into the inner magnetosphere and the auroral ionosphere. This is identified with the "unloading" energy input component extracted from observations, associated especially with the expansive phase of substorms, but there is also a so-called "directly driven" energy input component, in which (it must be assumed) energy is being added from the solar wind to the magnetotail at the same rate at which it is being withdrawn by dissipation and ring current buildup. (Despite the apparent connotations of the term "directly driven," the energy input even in this case always proceeds in two steps, via the magnetic field as an intermediary; it is just that the two conversions, from mechanical to electromagnetic and vice versa, both proceed at the same rate.)

The evidence for the "directly driven" component is, in essence, that the (observationally inferred) time history of the total power expended in the magnetosphere can be correlated, more or less closely, with the time history of a suitable function of solar wind parameters, often called the coupling function for the solar wind/magnetosphere interaction (of which there are several empirical or semi-empirical models [e.g., *Gonzalez*, 1990; *Gonzalez et al.*, 1994], the "epsilon function" of *Perreault and Akasofu* [1978] being probably the best known). There is, however, as yet no independent proof that any of these coupling functions really represents the rate at which solar wind mechanical energy is being converted to electromagnetic energy. An alternate interpretation is that the coupling function merely models the solar wind control of the energy output process (from magnetic energy of the magnetotail to the mechanical energy of ring current and auroral particles), while the energy input (from mechanical energy of the solar wind to magnetic energy of the magnetotail) may proceed at some other rate which at present is largely unknown, except perhaps for its grossest features.

Quantitatively, the rate of energy conversion between electromagnetic and mechanical forms is governed by the scalar product of electric field and current density. The energy flow into the ring current and auroral/ionospheric dissipation region ($\boldsymbol{E}\cdot\boldsymbol{J}$ positive) from the region of the energy source from the solar wind ($\boldsymbol{E}\cdot\boldsymbol{J}$ negative) can be readily traced with the Poynting vector or any of its several equivalents. Physically, the most important constraint is that, on the average, the region of negative $\boldsymbol{E}\cdot\boldsymbol{J}$ must have enough net inflow of solar wind mechanical energy to balance the net outflow of electromagnetic energy. The dominant energy of solar wind plasma in the relevant region is kinetic energy of bulk flow, and only a small fraction of that can be tapped because the plasma flows out of the region with a speed not much reduced below its initial value. Hence a large amount of solar wind plasma must be flowing through the interaction region that powers the magnetosphere: a rough estimate gives about 1/3 of the solar wind flow through an area equal to the cross section of the magnetotail [cf. *Vasyliunas*, 1987].

Most studies to date of the energy budget have not attempted to differentiate particularly between storms and substorms, except possibly for timescale and intensity. A recent result showing a significant qualitative difference between energy transfer in storms and in substorms [*Iyemori and Rao*, 1996] has been interpreted by *Siscoe and Petschek* [1997] as indicating a significant reduction in magnetic energy during a substorm expansion phase; this implies that energy dissipation during substorm expansion is fed largely from a reduction of magnetic energy, and thus the magnetospheric energy budget departs significantly from the average balance between solar wind mechanical input and electromagnetic output.

7.2. Comment on the Intensity of Magnetic Storms in Terms of the *Dst* Index

It has commonly been assumed that the intensity of magnetic storms can be defined by the minimum *Dst* value at the end of the main phase [*Sugiura and Chapman*, 1960; *Loewe and Prölss*, 1997; *Yokoyama and Kamide*, 1997]. The *Dst* index is defined as the symmetric or zonal part of magnetic disturbances, that is

$$D\,(\text{disturbance}) = Dst + DS$$

where *DS* is the local time dependent component of magnetic disturbances. *Sugiura* [1964] published hourly values of *Dst* for IGY: this parameter is currently computed/compiled by WDC-C2 in Kyoto and is widely used for research in geomagnetic storms. The intensity of *Dst*, i.e., the depression at the Earth's surface near the equator, represents the total energy of ring current particles in the 10 - 300 keV energy range, located between 2 and 8 R_E [*Dessler and Parker*, 1959; *Sckopke*, 1966].

It is the purpose of this subsection to point out that changes in the *Dst* index do not always monitor changes in the ring current surrounding the Earth. This is simply because currents other than the "symmetric" ring currents, such as field-aligned currents associated with the partial ring current, also contribute to the *Dst* index. Their relative importance varies from storm to storm, and even within one magnetic storm, it depends strongly on storm time.

In particular, one must exercise caution in using the currently-available hourly *Dst* values which are being derived from the *H* component perturbations at four widely separated midlatitude observatories. The magnetic perturbations at each observatory are corrected both for the *Sq* effects and for latitude, assuming that the *Sq* pattern does not change during magnetic storms and that magnetic perturbations at the Earth's surface are uniform so that the *H* component is proportional to cosine of latitude. A *Dst* value is the simple average of these four values. These assumptions are not valid, however, unless the ring current is purely "ring" and is located at a great distance from the Earth. Substorms are by no means symmetrical in local time, and intense substorms occur quite frequently during a magnetic storm. Thus the present *Dst* value includes significantly an artificially symmetric value resulting from asymmetric perturbations.

Figure 15 is a schematic diagram showing typical storm time *H* component variations at midlatitudes at four MLT sectors: 1200, 1800, 0000, and 0600 MLT. For simplicity, it is assumed that only one substorm takes place during the main phase, that the effects of the growth phase are negligible, and that the symmetric ring current grows and decays systematically in MLT. Superposed are the effects of the so-called substorm wedge current system [see *McPherron*, 1991]. It can clearly be seen that the substorm effect is characterized by positive and negative *H* perturbations, depending on MLT. The main sources generating the positive perturbations are field-aligned currents which constitute the wedge current system, as demonstrated by *Kamide and Fukushima* [1971] and *Crooker and Siscoe* [1974]. However, the partial ring current is the main contributor to the negative perturbation. The relative strength of these positive and negative perturbations depends on how widely (in local time) the wedge current system is distributed, which indeed changes considerably during a substorm. The average curve, which represents *Dst* by definition, is indicated by a dashed line. Therefore the positive change in *Dst* does not necessarily mean that the ring current decays but rather that the change is in fact caused by field-aligned currents and their associated current in the magnetotail. It can be argued that even though the *Dst* magnitude is decreasing in the main phase, the ring current, partial in this case, may in fact be growing associated with substorms expansion. It is thus misleading to state that the decrease in the *Dst* decrease rate reflects directly the decay of the

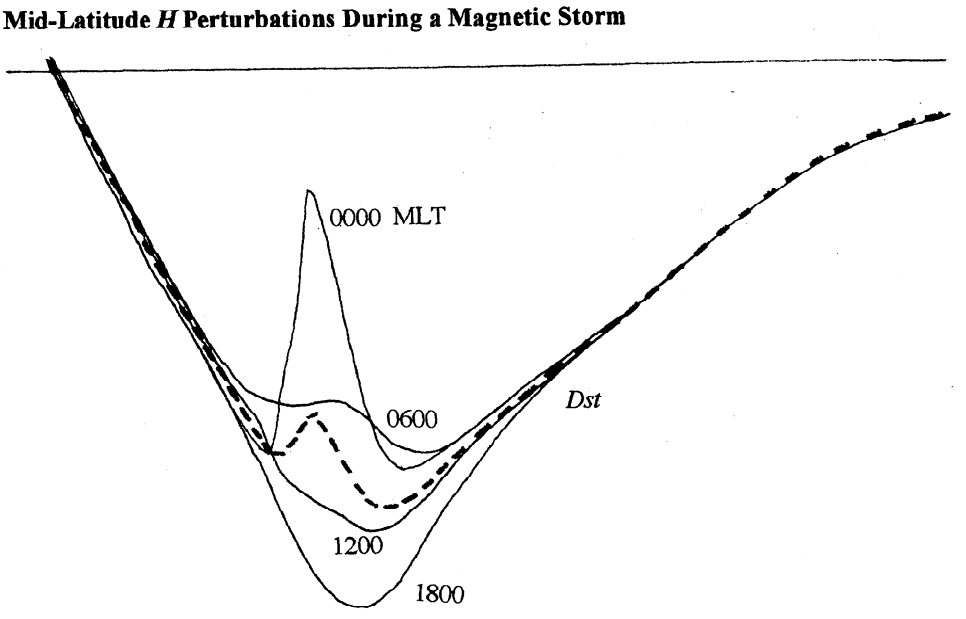

Figure 15. Schematic illustration of midlatitude magnetic variations in the H component at three different MLTs (magnetic local times) and the expected *Dst* variations.

ring current or that substorm occurrence does not contribute to the ring current [see *Iyemori and Rao*, 1996; *Rostoker et al.*, 1997].

8. Summary

The present review paper has attempted to clarify outstanding questions in the area of storm/substorm relationships. In fact, there are many controversies which have arisen as a consequence of the results of observational and modeling studies carried out over the last decade. The storm-substorm relationship is poorly understood, and some of the basic questions remain unsolved regarding the importance of frequently occurring intense substorms in a geomagnetic storm. In the following, we summarize our extensive discussions set forth in the present paper by presenting six major questions:

8.1. What are the Solar Wind Sources of Geomagnetic Storms?

Four mechanisms are shown to be the main sources of enhanced dawn-to-dusk electric fields of substantial duration in the interplanetary medium. They are ICMEs, CIRs, Alfvénic IMF fluctuations, and the Russell-McPherron effect. Of these, ICMEs and CIRs appear to be the primary sources leading to the development of magnetic storms. CMEs are impulsive solar/coronal ejecta that occur near the maximum sunspot phase of the solar cycle. Most geoeffective ICMEs are magnetic clouds, a subset of ejecta characterized by large north-south components of the IMF. During the declining phase of the solar cycle, coronal holes tend to dominate, expanding from the polar regions to equatorial locations. Fast plasma is continuously emitted from these coronal holes. CIRs, which consist of plasma and field compressions, are generated by the interaction of the fast solar wind stream and the slow stream.

The other two are "modulators" that generally do not drive magnetic storms without an ICME or CIR, but increase/decrease the geoeffectiveness of the ICMEs and CIRs effects through the different phases of individual geiomagnetic storms, the sunspot cycle, and seasons. HILDCAAs, typically occurring during the recovery phase of magnetic storms, are the effects of the Alfvénic trains in the IMF. The 22-year solar cycle dependence of geomagnetic activity must be quantitatively evaluated.

8.2. How Well Can Presently Available Numerical Schemes Predict Magnetic Storms?

Predictions of the growth and decay of geomagnetic storms using observations of solar wind conditions continue to be improved. Regardless of linear or nonlinear predictive techniques, it seems possible to reproduce most of the variance in the storm time *Dst* index directly from solar wind variables. This contrasts with the traditional view that substorms are essential to *Dst* evolution during the main phase of magnetic storms.

8.3. How are Storms and Substorms Coupled?

Of the two processes playing essential roles in enhancing the stormtime ring current, the electric field driven by southward IMF dominates the effects of the induced electric field in the magnetosphere resulting from substorm expansion onsets. There is, however, persuasive evidence in recent satellite observations that the constituents of the ring current show the greatest increases in their ionospheric components during the main phase of geomagnetic storms. The acceleration of these ions is presumably due to substorm-associated electric fields, indicating that the frequent occurrence of substorms is very important in forming the storm time ring current. This creates a new controversy regarding the relative importance of the two processes.

8.4. What is the Relative Importance of Ionospheric-Origin Ions and Solar Wind-Origin Ions in Constituting Ring Current Particles?

Changes in the large-scale electric field during magnetic storms, both substorm-related and directly driven by the solar wind, can trap particles well inside geosynchronous orbit. Recent satellite observations in the inner magnetosphere have shown, however, that the abundance of ionospheric origin ions (particularly O^+) is high and is highly correlated with substorm activity. This O^+ dominance coupled with the fact that a significant fraction of H^+ is also ionospheric in origin, suggests that the cause of the intense ring current during great storms is the enhanced outflow of ionospheric ions. Note, however, that the relative importance of ionospheric origin and solar wind origin ions varies considerably from storm to storm.

8.5. What Magnetospheric Processes Heat Ions to the Ring Current Energy?

Many questions remain unanswered with regard to the population of the ring current during magnetic storms and the loss process of ring current particles. One of the key issues is to differentiate between storm time substorms and nonstorm time substorms in terms of energy transport/conversion mechanisms in the magnetotail. It is particularly crucial to address the question of whether the difference between the two forms of substorms in the plasma sheet and the tail lobes, such as plasma injections and dipolarization at substorm expansion onsets, is simply a matter of size or of quality.

8.6. How Well does the Present *Dst* Index Represent the Strength of the Ring Current During Magnetic Storms?

The question of whether the *Dst* index is an accurate and effective measure of the storm-time ring current is also controversial. It is not well appreciated in the scientific community that variations in the *Dst* index do not always represent changes in the ring current encircling the Earth. They include the considerable influence of the partial ring current connected with field-aligned currents. It is also demonstrated that the dipolarization effect associated with substorm expansions acts to reduce the *Dst* magnitude, even when the ring current may still be growing.

Acknowledgments. We thank L. F. Bargatze, A. T. Y. Lui, and G. L. Siscoe for their illuminating discussions during the preparation of this manuscript. The work of Y. Kamide at the Solar-Terrestrial Environment Laboratory was supported by the Ministry of Education, Science, Sports, and Culture (Monbusho) under a Grant-in-Aid for Scientific Research, Category B. The work of R. L. McPherron was supported in part by grants by the National Science Foundation (NSF) ATM-95-02124 and the National Aeronautics and Space Administration (NASA) NAG5-1167. Work by J. L. Phillips was performed at the Solar-Terrestrial Environment Laboratory as a visiting faculty member. The work of G. Rostoker was supported by the Natural Sciences and Engineering Research Council of Canada. The work of A. S. Sharma at the University of Maryland is supported by National Science Foundation grants ATM-9626622 and ATM-9713479, and NASA grants NAGW-3596 and NAGS-1101. Portions of this research were performed at the Jet Propulsion Laboratory, California Institute of Technology under contract with NASA.

The Editor thanks Syun-Ichi Akasofu and another referee for their assistance in evaluating this paper.

References

Akasofu, S.-I., The development of geomagnetic storms without a preceding enhancement of the solar plasma pressure, *Planet. Space Sci., 13*, 297, 1965.

Akasofu, S.-I., *Polar and Magnetospheric Substorms*, D. Reidel, Norwell, Mass.,, 1968.

Akasofu S.-I., The energy coupling between the solar wind and the magnetosphere, *Space Sci. Rev., 28*, 121, 1981.

Akasofu, S.-I., and S. Chapman, The ring current, geomagnetic disturbance and the Van Allen radiation belts, *J. Geophys. Res., 66*, 1321, 1961.

Akasofu, S.-I., S. DeForest, and C. E. McIlwain, Auroral displays near the "foot" of the field line of the ATS-5 satellite, *Planet. Space Sci., 22*, 25, 1974.

Alfvén, H., On the solar origin of cosmic radiation, *Phys. Rev., 75*, 1732, 1949.

Baker, D. N., Statistical analysis in the study of solar wind-magnetosphere coupling, in *Solar Wind-Magnetosphere Coupling*, edited by Y. Kamide and J. A. Slavin, p. 17, Terra Sci., Tokyo, 1986.

Balsiger, H., P. Eberhardt, J. Geiss, and D. T. Young, Magnetic storm injection of 0.9- to 16-keV/*e* solar and terrestrial ions into the high-altitude magnetosphere, *J. Geophys. Res., 85*, 1645, 1980.

Bargatze, L. F., D. N. Baker, R. L. McPherron, and E. W. Hones, Jr., Magnetospheric response for many levels of geomagnetic activity, *J. Geophys. Res., 90*, 6385, 1985.

Bartels, J. Terrestrial-magnetic activity and its relations to solar phenomena, *J. Geophys. Res., 37*, 1, 1932.

Baumjohann, W., Near-Earth plasma sheet dynamics, *Adv. Space Res., 18(10)*, 27, 1996.

Baumjohann, W., Y. Kamide, and R. Nakamura, Substorms, storms, and the near-Earth tail, *J. Geomagn. Geoelectr., 48*, 177, 1996.

Belcher, J. W., and L. Davis Jr., Large amplitude Alfvén waves in the interplanetary medium, *J. Geophys. Res., 76*, 3534, 1971.

Burton, R. K., R. L. McPherron, and C. T. Russell, An empirical relationship between interplanetary conditions and *Dst*, *J. Geophys. Res., 80*, 4204, 1975.

Campbell, W. H., Geomagnetic storms, the *Dst* ring-current myth, and lognormal distributions, *J. Atmos. Terr. Phys., 58*, 1171, 1996.

Casdagli, M., A dynamical system approach to modeling input-output systems, in *Nonlinear Modeling and Forecasting*, edited by M. Casdagli and S. Eubanks, p. 265, Addison-Wesley, Reading, Mass., 1992.

Chapman, S., and J. Bartels, *Geomagnetism*, Vol. 1, Chap. IX, Clarendon, Oxford, 1940.

Chapman, S., and V. C. A. Ferraro, A new theory of magnetic storms, *J. Geophys. Res., 36*, 171, 1931.

Chen, J., P. J. Cargill, and P. J. Palmadesso, Real-time identification and prediction of geoeffective solar wind structures, *Geophys. Res. Lett., 23*, 625, 1996.

Chen, J., P. J. Cargill, and P. J. Palmadesso, Predicting solar wind structures and their geoeffectiveness, *J. Geophys. Res., 102*, 14701, 1997.

Clauer, C. R., The technique of linear prediction filters applied to studies of solar wind-magnetosphere coupling, in *Solar Wind-Magnetosphere Coupling*, edited by Y. Kamide and J. A. Slavin, p. 39, Terra Sci., Tokyo, 1986.

Cliver, E. W., V. Boriakoff, and K. H. Bounar, The 22-yr cycle of geomagnetic and solar wind activity, *J. Geophys. Res., 101*, 27091, 1996.

Costello, K. A., Retraining neural networks for the prediction of *Dst* in the Rice Magnetospheric Specification and Forecast Model, M.S. thesis, Rice Univ., Houston, Tex., 1996.

Cowley, S. W. H., The role and location of magnetic reconnection in the geomagnetic tail during substorms, *Eur. Space Agency Spec. Publ., ESA-SP, 335*, 401-404, 1992.

Crooker, N. U., and E. W. Cliver, Reply, *Geophys. Res. Lett., 20*, 1661, 1993.

Crooker, N. U. and E. W. Cliver, Postmodern view of M-regions, *J. Geophys. Res., 99*, 23383, 1994.

Crooker, N. U., and G. L. Siscoe, Model geomagnetic disturbance from asymmetiric ring current particles, *J. Geophys. Res., 79*, 589, 1974.

Crooker, N. U., E. W. Cliver, and B. T. Tsurutani, The semiannual variation of great geomagnetic storms and the postshock Russell-McPherron effect preceding coronal mass ejecta, *Geophys. Res. Lett., 19*, 429, 1992.

Daglis, I. A., The role of magnetosphere-ionosphere coupling in magnetic storm dynamics, in *Magnetic Storms, Geophys. Monogr. Ser.*, vol. 98, edited by B. T. Tsurutuani, W. D. Gonzalez, Y. Kamide, and J. K. Arballo, 107-116, AGU, Washington, D.C., 1997.

Daglis, I. A., S. Livi, E. T. Sarris, and B. Wilken, Energy density of ionospheric and solar wind origin ions in the near-Earth magnetotail during substorms, *J. Geophys. Res., 99*, 5691-5703, 1994.

Daglis, I. A., E. T. Sarris, G. Kremser, and B. Wilken, On the solar wind-magnetosphere-ionosphere coupling: AMPTE/CCE particle data and the *AE* indices, in *Study of the Solar-Terrestrial System, Eur. Space Agency Spec. Publ., ESA SP-346*, 193-198, 1992.

Daglis, I. A., W. I. Axford, S. Livi, B. Wilken, M. Grande, and F. Søraas, Auroral ionospheric ion feeding of the inner plasma sheet during substorms, *J. Geomagn. Geoelectr., 48*, 729-739, 1996.

Dessler, A. J., and E. N. Parker, Hydromagnetic theory of magnetic storms, *J. Geophys. Res., 64*, 2239, 1959.

Detman, T. R., and D. Vassiliadis, Review of techniques for magnetic storm forecasting, in *Magnetic Storms, Geophys. Monogr. Ser.*, vol. 98, edited by B. T. Tsurutani, W. D. Gonzalez, Y. Kamide, and J. K. Arballo, p. 253, AGU, Washington, D. C., 1997.

Farmer, J. D., and J. J. Sidorowich, Predicting chaotic time series, *Phys. Rev. Lett., 59*, 845, 1987.

Farrugia, C. J., L. F. Burlaga, and R. P. Lepping, Magnetic clouds and the quiet-storm effect at Earth, in *Magnetic Storms, Geophys. Monogr.*

Ser., vol. 98, edited by B. T. Tsurutani, W. D. Gonzalez, Y. Kamide, and J. K. Arballo, p. 91, AGU, Washington, D. C., 1997.

Fay, R. A., C. R. Garrity, R. L. McPherron, and L. F. Bargatze, Prediction filters for the *Dst* index and the polar cap potential, in *Solar Wind-Magnetosphere Coupling*, edited by Y. Kamide and J. A. Slavin, p. 111, Terra Sci., Tokyo, 1986

Feldstein, Y. I., V. Y. U. Pisarsky, N. M. Rudneva and A. Grafe, Ring current simulation in connection with interplanetary space conditions, *Planet. Space Sci., 32*, 975, 1984.

Frank, L. A., On the extraterrestrial ring current during geomagnetic storms, *J. Geophys. Res., 72*, 3753, 1967.

Freeman, J., A. Nagai, P. Reiff, W. Denig, S. Gussenhoven-Shea, M. Heinemann, F. Rich, and M. Hairston, The use of neural networks to predict magnetospheric parameters for input to a magnetospheric forecast model, in *Artificial Intelligence Applications in Solar Terrestrial Physics*, edited by J. Joselyn, H. Lundstedt and Trollinger, 167, Natl. Oceanic and Atmos. Admin., Boulder, Colo., 1994.

Gleisner, H., and H. Lundstedt, Response of the auroral electrojets to the solar wind modeled with neural networks, *J. Geophys. Res., 102*, 14269, 1997.

Gloeckler, G., and D. C. Hamilton, AMPTE ion composition results, *Phys. Scr., T18*, 73, 1987.

Goertz, C. K., L.-H. Shan, and R. A. Smith, Prediction of geomagnetic activity, *J. Geophys. Res., 98*, 7673, 1993.

Gonzalez, W. D., A unified view of solar wind - magnetosphere coupling functions, *Planet. Space Sci., 38*, 627, 1990.

Gonzalez, W. D., and F. S. Mozer, A quantitative model for the potential resulting from reconnection with an arbitrary interplanetary magnetic field, *J. Geophys. Res., 79*, 4186, 1974.

Gonzalez, W., and B. T. Tsurutani, Criteria of interplanetary parameters causing intense magnetic storms, *Planet. Space Sci., 35*, 1101, 1987.

Gonzalez, W. D., B. T. Tsurutani, A. L. C. Gonzalez, E. J. Smith, F. Tang, and S.-I. Akasofu, Solar wind-magnetosphere coupling during intense magnetic storms (1978-1979), *J. Geophys. Res., 94*, 8835, 1989.

Gonzalez, W. D., A. L. C. Gonzalez, and B. T. Tsurutani, Dual-peak solar cycle distribution of intense geomagnetic storms, *Planet. Space. Sci., 38*, 181, 1990.

Gonzalez, W. D., A. L. C. Gonzalez, and B. T. Tsurutani, Comment on "The semiannual variation of great geomagnetic storms and the postshock Russell-McPherron effect preceding coronal mass ejecta," *Geophys. Res. Lett., 20*, 1659, 1993.

Gonzalez, W. D., J. A. Joselyn, Y. Kamide, H. W. Kroehl, G. Rostoker, B. T. Tsurutani, and V. M. Vasyliunas, What is a geomagnetic storm?, *J. Geophys. Res., 99*, 5771, 1994.

Gosling, J. T., D. N. Baker, S. J. Bame, W. C. Feldman, R. D. Zwickl, and E. J. Smith, Bi-directional solar wind electron heat flux events, *J. Geophys. Res., 92*, 8519, 1987.

Gosling, J. T., D. J. McComas, J. L. Phillips, and S. J. Bame, Geomagnetic activity associated with Earth passage of interplanetary shock disturbances and coronal mass ejections, *J. Geophys. Res., 96*, 7831, 1991.

Green, C. A., The Semiannual variation in the magnetic activity indices A_a and A_p, *Planet. Space Sci., 32*, 297, 1984.

Henderson, M. G., G. D. Reeves, H. E. Spence, R. B. Sheldon, A. M. Jorgensen, J. B. Blake, and J. F. Fennell, First energetic neutral atom images from Polar, *Geophys. Res. Lett., 24*, 1167, 1997.

Hernandez, J. V., T. Tajima, and W. Horton, Neural net forecasting geomagnetic activity, *Geophys. Res., Lett., 20*, 2707, 1993.

Hamilton, D. C., G. Gloeckler, F. M. Ipavich, W. Studemann, B. Wilken, and G. Kremser, Ring current development during the great geomagnetic storm of February 1986, *J. Geophys. Res., 93*,14343, 1988.

Hill, T. W., Origin of the plasma sheet, *Rev. Geophys., 12*, 379, 1974.

Hill, T. W., Rates of mass, momentum and energy transfer at the magnetopause, in *Magnetospheric Boundary Layers, Eur. Space Agency Spec. Publ., ESA SP-148*, 325, 1979.

Ho, C. M., and B. T. Tsurutani, The distant tail behavior during high speed solar wind streams and magnetic storms, *J. Geophys. Res., 102*, 14165, 1997.

Hones, E. W., Jr., Plasma sheet behavior during substorms; in *Magnetic Reconnection in Space and Laboratory Plasmas, Geophys. Monogr. Ser.*, vol. 30, edited by E. W. Hones Jr., p. 178, AGU, Washington, D.C., 1984.

Huang, C. Y., L. A. Frank, G. Rostoker, J. Fennell, and D. G. Mitchell, Nonadiabatic heating of the central plasma sheet at substorm onset, *J. Geophys. Res., 97*, 1481, 1992.

Hultqvist, B., On the acceleration of positive ions by high-latitude, large amplitude electric field fluctuations, *J. Geophys. Res., 101*, 27111, 1996.

Hultqvist, B., R. Lundin, K. Stasiewicz, L. Block, P.-A. Lindquist, G. Gustafsson, H. Koskinen, A. Bahnsen, T. A. Potemra, and L. J. Zanetti, Simultaneous observations of upward moving field-aligned electrons and ions on auroral zone field lines, *J. Geophys. Res., 93*, 9765-9776, 1988.

Hundhausen, A. J., J. T. Burkepile, and O. C. St. Cyr, Speeds of coronal mass ejections: SMM observations from 1980 and 1984-1989, *J. Geophys. Res., 99*, 6543, 1994.

Iyemori, T., and D. R. K. Rao, Decay of the *Dst* field of geomagnetic disturbance after substorm onset and its implication to storm-substorm relations, *Ann. Geophys., 14*, 6087, 1996.

Iyemori, T., H. Maeda, and T. Kamei, Impulse response of geomagnetic indices to interplanetary magnetic fields, *J. Geomagn. Geoelectr., 31*, 1, 1979.

Jacquey, C., J. A. Sauvaud, and J. Dandouras, Location and propagation of the magnetotail current disruption during substorm expansion: Analysis and simulation of an ISEE multi-onset event, *Geophys. Res. Lett., 18*, 389, 1991.

Johnson, R. G., R. D. Sharp, and E.G. Shelley, Observations of ions of ionospheric origin in the storm-time ring current, *Geophys. Res. Lett., 4*, 403, 1977.

Joselyn, J. A., Geomagnetic activity forecasting: The state of the art, *Rev. Geophys., 33*, 383, 1995.

Joselyn, J. A., and B. T. Tsurutani, Geomagnetic sudden impulses and storm sudden commencements, *Eos Trans. AGU, 71*, 1808,, 1990.

Kamide, Y., Relationship between substorms and storms, in *Dynamics of the Magnetosphere*, edited by S.-I. Akasofu, p. 425, D. Reidel, Norwell, Mass., 1979.

Kamide, Y., Is substorm occurrence a necessary condition for a magnetic storm?, *J. Geomagn. Geoelectr., 44*, 109, 1992.

Kamide, Y., and J. H. Allen, Some outstanding problems of the storm/substorm relationship, in *Proceedings of Solar Terestrial Predictions Workshop V*, edited by G. Heckman, K. Marubashi, M. A. Shea, D. F. Smart, and T. Thompson, p. 207, RWC Tokyo, Tokyo, 1997.

Kamide, Y., and N. Fukushima, Analysis of magnetic storms with *DR*-indices for equatorial ring current field, *Rep. Ionos. Space Res., Jpn., 26*, 79, 1971.

Kamei, T., and M. Sugiura, A plan on derivation of a near real-time *Dst* index, *IAGA News*, 35, 47, Boulder, Colo., 1996.

Kan, J. R., L. Zhu, and S.-I. Akasofu, A theory of substorms: Onset and subsidence; *J. Geophys. Res., 93*, 5624, 1988.

Klein, L. W., and L. F. Burlaga, Magnetic clouds at 1 AU, *J. Geophys. Res., 87*, 613, 1982.

Klimas, A. J., D. Vassiliadis, D. N. Baker, and D. A. Roberts, The organized nonlinear dynamics of the magnetosphere, *J. Geophys. Res., 101*, 13089, 1996.

Knipp, D. J., and B. A. Emery, A report on the community study of the early November 1993 geomagnetic storm, *Adv. Space Res., 20(5)*, 895, 1997.

Kozyra, J. U., V. K. Jordanova, R. B. Horne, and R. M. Thorne, Modeling of the contribution of electromagnetic ion cyclotron (EMIC) waves to storm time ring current erosion, in *Magnetic Storms, Geophys. Monogr. Ser.* vol. 98, edited by B. T. Tsurutani, W. D. Gonzalez, Y. Kamide, and J. K. Arballo, p. 187, AGU, Washington, D. C., 1997.

Krimigis, S. M., G. Haerendel, R. W. McEntire, G. Paschmann, and D. A. Bryant, The active magnetospheric particle tracer explorers (AMPTE) program, *Eos Trans. AGU, 63*, 843, 1982.

Liu, W. W., and G. Rostoker, Energetic ring current particles generated by recurring substorm cycles, *J. Geophys. Res., 100*, 21897, 1995.

Loewe, C. A., and G. W. Prölss, Classification and mean behavior of magnetic storms, *J. Geophys. Res., 102*, 14209, 1997.

Lui, A. T. Y., R. E. Lopez, S. M. Krimigis, R. W. McEntire, L. J. Zanetti, and T. A. Potemra, A case study of magnetotail current sheet disruption and diversion, *Geophys. Res. Lett., 15*, 721, 1988.

Lundin, R., and B. Hultqvist, Ionospheric plasma-escape by high altitude electric fields: Magnetic moment pumping, *J. Geophys. Res., 94*, 6665, 1989.

Lundin, R, L. Eliasson, and K. Stasiewicz, Plasma energization on auroral field lines as observed by the Viking spacecraft, *Geophys. Res. Lett., 14*, 443, 1987.

Lundin, R., G. Gustafsson, A. I. Eriksson, and G. T. Marlund, On the importance of high-altitude low-frequency electric fluctuations for the escape of ionospheric ions, . *Geophys. Res., 95,* 5905, 1990.

Lundstedt, H., AI techniques in geomagnetic storm forecasting, in *Magnetic Storms. Geophys. Monogr. Ser.*, vol., 98, edited by B. T. Tsurutani, W. D. Gonzalez, Y. Kamide, and J. K. Arballo, p. 243, AGU, Washington, D. C., 1997.

McComas, D. J., J. T. Gosling, S. J. Bame, E. J. Smith, and H. V. Cane, A test of magnetic field draping induced B_Z perturbations ahead of fast coronal mass ejecta, *J. Geophys. Res., 94,* 1465, 1989.

McPherron R. L., Physical processes producing magnetospheric substorms and magnetic storms, in *Geomagnetism,* vol. 4, p. 594, Academic, San Diego, Calif. , 1991.

McPherron, R. L., The role of substorms in the generation of magnetic storms, in *Magnetic Storms, Geophys. Monogr. Ser.*, vol. 98, edited by B. T. Tsurutani, W. D. Gonzalez, Y. Kamide, and J. K. Arballo, p. 131, AGU, Washington, D. C., 1997.

McPherron, R. L., and G. Rostoker, Comment on "Prediction of geomagnetic activity" by C. K. Goertz, L.-H. Shan, and R. A. Smith, *J. Geophys. Res., 98,* 7685, 1993.

McPherron, R. L., C. T. Russell, and M. P. Aubry, Satellite studies of magnetospheric substorms on August 15, 1968, 9, Phenomenological model for substorms, *J. Geophys. Res., 78,* 3131, 1973.

McPherron, R. L., D. N. Baker, and L. F. Bargatze, Linear filters as a method of real time prediction of geomagnetic activity, in *Solar Wind-Magnetosphere Coupling*, edited by Y. Kamide and J. A. Slavin, p. 85, Terra Sci., Tokyo, 1986.

Maezawa, K., and T. Murayama, Solar wind velocity effects on the auroral zone magnetic disturbances, in *Solar Wind-Magnetosphere Coupling*, edited by Y. Kamide and J. A. Slavin, p. 59, Terra Sci., Tokyo, 1986.

Murayama, T., Coupling functions between the solar wind and *Dst* index, in *Solar Wind-Magnetosphere Coupling*, edited by Y. Kamide and J. A. Slavin, p. 111, Terra Sci., Tokyo, 1986.

National Space Weather Program Strategic Plan, Office of the Federal Coordinator for Meteorological Services and Supporting Research, *Rep. FCM-P30-1995*, Washington, D. C., 1995.

National Space Weather Program Implementation Plan, Office of the Federal Coordinator for Meteorological Services and Supporting Research, Washington, D. C., 1997.

Neupert, W. M., and V. Pizzo, Solar coronal holes as sources of recurrent geomagnetic disturbances, *J. Geophys. Res., 79,* 3701, 1974.

Ohtani, S., S. Kokubun, and C. T. Russell, Radial expansion of the tail current disruption during substorms: A new approach to the substorm onset region, *J. Geophys. Res., 97,* 3129, 1992.

Packard N. H., J. P. Crutchfield, J. D. Farmer, and R. S. Shaw, Geometry from a time series, *Phys. Rev. Lett., 45,* 712, 1990.

Perreault, P. D., and S.-I. Akasofu, A study of geomagnetic storms, *Geophys. J. R. Astron. Soc., 54,* 547, 1978.

Phillips, J. L., J. T. Gosling, and D. J. McComas, Coronal mass ejections and geomagnetic storms: Seasonal variations, in *Solar Terrestrial Predictions IV*, vol. 3, edited by J. Hruska, M. A. Shea, D. F. Smart, and G. Heckman, p. 242, Natl. Oceanic and Atmos. Admin., Boulder, Colo., 1993.

Phillips, J. L., S. J. Bame, W. C. Feldman, B. E. Goldstein, J. T. Gosling, C. M. Hammond, D. J. McComas, M. Neugebauer, E. E. Scime, and S. T. Suess, Ulysses solar wind plasma observations at high southerly latitudes, *Science, 268,* 1030, 1995.

Price C. P., D. Prichard, and J. E. Bischoff, Nonlinear input-output analysis of auroral electrojet index, J. *Geophys. Res., 99,* 13227, 1994.

Prölss, G. W., Decay of the magnetic storm ring current by charge-exchange mechanism, *Planet. Space Sci. , 21,* 983, 1973.

Reeves, G. D., R. W. H. Friedel, M. G. Henderson, A. Korth, P. S. McLachlan, and R.D. Belian, Radial propagation of substorm injections, in *Substorms 3, ESA SP-339*, p. 579, 1996.

Rosenberg, R. L. and P. J. Coleman, Heliographic latitude dependence of the dominant polarity of the interplanetary magnetic field, *J. Geophys. Res., 74,* 5611, 1969.

Rostoker, G., and C.-G. Fälthammar, Relationship between changes in the interplanetary magnetic field and variations in the magnetic field at the Earth's surface, *J. Geophys. Res., 72,* 5853, 1967.

Rostoker, G., W. Baumjohann, W. Gonzalez, Y. Kamide, S. Kokubun, R. L. McPherron, and B. T. Tsurutani, Comment on "Decay of the *Dst* field of geomagnetic disturbance after substorm onset and its implication to storm-substorm relations," by Iyemori and Rao, *Ann. Geophys, 15,* 848, 1997.

Russell, C. T., and R. M. McPherron, Semiannual variation of geomagnetic activity, *J. Geophys. Res., 78,* 92, 1973.

Russell, C. T., R. L. McPherron, and P. K. Burton, On the cause of geomagnetic storms, *J. Geophys. Res., 79,* 1105, 1974.

Sckopke, N., A general relation between the energy of trapped particles and the disturbance field near the Earth, *J. Geophys. Res., 71,* 3125, 1966.

Sharma A. S., Assessing the magnetosphere's nonlinear behavior retain: Its dimension is low, its predictability high, *U.S. Natl. Rep. Int. Union Geod. Geophys. 1991-1994, Rev. Geophys., 33,* 645, 1995.

Sheeley, N. R. Jr., J. W. Harvey, and W. C. Feldman, Coronal holes, solar wind streams, and recurrent geomagnetic disturbances, 1973-1976, *Solar Phys., 49,* 271, 1976.

Singer, S. F., A new model of magnetic storms and aurorae, *Eos Trans., AGU, 38,* 175, 1957.

Siscoe, G. L., and H. E. Petschek, On storm weakening during substorm expansion phase, *Ann. Geophysicae, 15,* 211-216, 1997.

Slavin, J. A., G. Jungman, and E. J. Smith, The interplanetary magnetic field during solar cycle 21: ISEE-3/ICE observations, *Geophys. Res. Lett., 13,* 513, 1986.

Smith, E. J. and J. H. Wolfe, Observations of interaction regions and corotating shocks between one and five *AU*: Pioneers 10 and 11, *Geophys. Res. Lett., 3,* 137, 1976.

Smith, P. H., and N. K. Bewtra, Charge exchange lifetimes for ring current ions, *Space Sci. Rev., 22,* 301, 1978.

Smith, P. H., and R. A. Hoffman, Ring current particle distribution during the magnetic storm of December 16-18, 1971, *J. Geophys. Res., 78,* 4731, 1973.

Stern, D. P., Energetics of the magnetosphere, *Space Sci. Rev., 39,* 193, 1984.

Sugiura, M., Hourly values of equatorial *Dst* for the IGY, *Ann. Int. Geophys. Year, 35,* 9, 1964.

Sugiura, M., and S. Chapman, The average morphology of geomagnetic storms with sudden commencement, *Abandl. Akad. Wiss., Gottingen Math. Phys. Kl,* no. 4, 1960.

Takens F., Detecting strange attractors in turbulence, in *Dynamical Systems and Turbulence*, edited by A. Dold and B. Eckmann, p. 366, Springer-Verlag, New York, 1981.

Taylor, J. R., M. Lester, and T. K. Yeoman, A superposed epoch analysis of geomagnetic storms, *Ann. Geophys., 12,* 612, 1994.

Taylor, J. R., M. Lester, and T. K. Yeoman, Seasonal variations in the occurrence of geomagnetic storms, *Ann. Geophys, 14,* 286, 1996.

Tsurutani, B. T., and W. D. Gonzalez, The cause of high-intensity long-duration continuous *AE* activity (HILDCAAS): Interplanetary Alfvén wave trains, *Planet. Space Sci. , 35,* 405, 1987.

Tsurutani, B. T., and W. D. Gonzalez, The efficiency of "viscous interaction" between the solar wind and the magnetosphere during intense northward IMF events, *Geophys. Res. Lett., 22,* 663, 1995.

Tsurutani, B. T., and W. D. Gonzalez, The interplanetary causes of magnetic storms: A Review, in *Magnetic Storms, Geophys. Monogr. Ser.*, vol. 98, edited by B. T. Tsurutani, W. D. Gonzalez, Y. Kamide, and J. K. Arballo, p. 77, AGU, Washington, D. C., 1997.

Tsurutani, B. T., B. E. Goldstein, W. D. Gonzalez, and F. Tang, Comment on "A new method of forecasting geomagnetic activity and proton showers," by A. Hewish and P. J. Duffet-Smith, Planet. *Space Sci., 36,* 205, 1988a.

Tsurutani, B. T., W. D. Gonzalez, F. Tang, S.-I. Akasofu, and E. J. Smith, Origin of interplanetary southward magnetic fields responsible for major magnetic storms near solar maximum (1978-1979), *J. Geophys. Res., 93,* 8519, 1988b.

Tsurutani, B. T., W. D. Gonzalez, F. Tang, and Y. T. Lee, Great magnetic storms, *Geophys. Res. Lett., 19,* 73, 1992.

Tsurutani, B. T., W. D. Gonzalez, A. L. C. Gonzalez, F. Tang, J. K. Arballo, and M. Okada, Interplanetary origin of geomagnetic activity in the declining phase of the solar cycle, *J. Geophys. Res., 100,* 21717, 1995.

Valdivia, J. A., A. S. Sharma, and K. Papadopoulos, Prediction magnetic storms by nonlinear dynamical models, *Geophys. Res. Lett., 23,* 2899, 1996.

Vassiliadis, D., A. J. Klimas, D. N. Baker, and D. A. Roberts, A description of the solar wind-magnetosphere coupling based on nonlinear prediction filters, *J. Geophys. Res., 100,* 3495, 1995.

Vasyliunas, V. M., Contribution to Dialog on the relative roles of reconnection and the "viscous" interaction in providing solar-wind energy to the magnetosphere, in *Magnetotail Physics*, edited by A. T. Y. Lui, p. 411, Johns Hopkins Univ. Press, Laurel, Md., 1987.

Vasyliunas, V. M., J. R. Kan, G .L. Siscoe, and S.-I. Akasofu, Scaling relations governing magnetospheric energy transfer, *Planet. Space Sci., 30*, 359, 1982.

Webb, D. F., Solar and geomagnetic disturbances during the declining phase of recent solar cycles, *Adv. Space Res., 16(9)*, 57, 1995.

Webb, D. F. and R. A. Howard, The solar cycle variation of coronal mass ejections and the solar wind mass flux, *J. Geophys. Res., 99*, 4201, 1994.

Weiss, L. A., P. H. Reiff, J. J. Moss, R. A. Heelis, and B. D.. Moore, Energy dissipation in substorms, in *Substorms 1*, *Eur. Space Agency Spec. Publ. ESA SP-335*, p. 309, 1992.

Wilken, B., I. A. Daglis, and S. Livi, Observations of geomagnetic storms by the CRRES satellite, *Eos Trans. AGU, 73*, 457, 1992a.

Wilken, B., W. Weiss, D. Hall, M. Grande, F. Soraas, and J. F. Fennell, Magnetospheric ion composition spectrometer onboard the CRRES spacecraft, *J. Spacecr. Rockets, 29*. 585, 1992b.

Williams, D. J., Ring current composition and sources, in *Dynamics of the Magnetosphere*, edited by S.-I. Akasofu, p. 407, D. Reidel, Norwell, Mass., 1980.

Williams, D. J., The Earth's ring current: Causes, generation, and decay, *Space Sci. Rev., 34*, 223, 1983.

Williams, D. J., Ring current and radiation belts, *Rev. Geophys., 25*, 570, 1987.

Wilson, R. M., On the behavior of the *Dst* geomagnetic index in the magnetic cloud passage at Earth, *J. Geophys. Res., 95*, 215, 1990.

Winterhalter, D., E. J. Smith, M. E. Burton, N. Murphy, and D. J. McComas, The heliospheric plasma sheet, *J. Geophys. Res., 99*, 6667, 1994.

Wodnicka, E. B. , What does the magnetic storm development depend on?, *Planet. Space Sci., 39*, 1163, 1991.

Wu, J.-G., and H. Lundstedt, Prediction of geomagnetic storms from solar wind data using Elman recurrent neural networks, *Geophys. Res. Lett., 23*, 319, 1996.

Wu, J.-G., and H. Lundstedt, Geomagnetic storm predictions from solar wind data with the use of dynamic neural networks, *J. Geophys. Res., 102*, 14255, 1997.

Yokoyama, N., and Y. Kamide, Statistical nature of geomagnetic storms, *J. Geophys. Res., 102*, 14215, 1997.

Zhao, X. P., J. T. Hoeksema, J. T. Gosling, and J. L. Phillips, Statistics of IMF B_z events, in *Solar Terrestrial Predictions IV*, vol. *3*, edited by J. Hruska, M. A. Shea, D. F. Smart, and G. Heckman, p. 712, Natl. Oceanic and Atmos. Admin., Boulder, Colo., 1993.

W. Baumjohann, Max-Planck-Institut für extraterrestrische Physik, D-85740 Garching, Germany. (e-mail: bj@mpe-garching.mpg.de)

I. A. Daglis, Institute of Ionospheric and Space Research, National Observatory of Athens, 15236 Penteli, Greece. (e-mail: daglis@creator.space.noa.gr)

W. D. Gonzalez, Instituto de Pesquisas Espaciais, São José dos Campos, São Paulo, Brazil. (e-mail: gonzalez@dge.inpe.br)

M. Grande, Rutherford Appleton Laboratory, Chilton, Didcot, Oxon OX11 0QX England, United Kingdom. (e-mail: M.Grande@rl.ac.uk)

J. A. Joselyn and H. J. Singer, Space Environment Center, NOAA, Boulder, CO 80303. (e-mail: jjoselyn@sec.noaa.gov; hsinger@sec.noaa.gov)

Y. Kamide, Solar-Terrestrial Environment Laboratory, Nagoya University, Toyokawa 442, Japan. (e-mail: kamide@stelab.nagoya-u.ac.jp)

R. L. McPherron, Institute of Geophysics and Planetary Physics, University of California, Los Angeles, CA 90024. (e-mail: rmcpherron@igpp.ucla.edu)

J. L. Phillips, NASA Johnson Space Center, Mail Code CB, Houston, TX 77059. (e-mail: JLPhilli@ems.jsc.gov)

E. G. D. Reeves, Los Alamos National Laboratory, Los Alamos, NM 87545. (e-mail: reeves@lanl.gov)

G. Rostoker, Department of Physics, University of Alberta, Edmonton, Alberta, Canada T6G 2J1. (e-mail: rostoker@space.ualberta.ca)

A. S. Sharma, Department of Astronomy, University of Maryland, College Park, MD 20742. (e-mail: ssh@avl.umd.edu)

B. T. Tsurutani, Jet Propulsion Laboratory, California Institute of Technology, Pasadena, CA 91109. (e-mail: btsurutani@jplsp.jpl.nasa.gov)

V. M. Vasyliunas, Max-Planck-Institut für Aeronomie, D-37189 Katlenburg-Lindau, Germany. (e-mail: vasyliunas@linax1.mpae.gwdg.de)

(Received July 16, 1997; revised March 18, 1998;
accepted March 24, 1998.)